

Active Brownian Particle and Random Walk Theories of the Motions of Zooplankton: Application to Experiments with Swarms of *Daphnia*

Udo Erdmann^{a,*}, Werner Ebeling^a, Lutz Schimansky-Geier^a,
Anke Ordemann^b, Frank Moss^b

^a*Institute of Physics, Humboldt-University Berlin, 12489 Berlin, Newtonstr. 15,
Germany*

^b*Center for Neurodynamics, University of Missouri at St. Louis, St. Louis, MO
63121, USA*

Abstract

Active Brownian Particles are self-propelled particles that move in a dissipative medium subject to random forces, or “noise”. Additionally, they can be confined by an external field and/or they can interact with one another. The external field may actually be an attractive marker, for example a light field (as in the experiment) or an energy potential or a chemical gradient (as in the theory). The potential energy can also be the result of interparticle attractive and/or repulsive forces summed over all particles (a mean field potential). Four, qualitatively different motions of the particles are possible: at small particle density their motions are approximately independent of one another subject only to the external field and the noise, which results in moving randomly through or performing rotational motions about a central point in space. At increasing densities interactions play an important role and individuals form a swarm performing several types of self-organized collective motion. We apply this model for the description of zooplankton *Daphnia* swarms. In the case of the zooplankton *Daphnia* (and probably many other aquatic animals that form similar motions as well) this vortex is hydrodynamical but motivated by the self-propelled motion of the individuals. Similar vortex-type motions have been observed for other creatures ranging in size from bacteria to flocks of birds and schools of fish. However, our experiment with *Daphnia* is unique in that all four motions can be observed in controlled laboratory conditions with the same animal. Moreover, the theory, presented in both continuous differential equation and random walk forms, offers a quantitative, physically based explanation of the four motions.

Key words: Active motion, self-propelled particles, vortex motion, noise-induced bifurcation, symmetry breaking, Zooplankton

1 Introduction

The theory of Active Brownian Particles (ABP) has been developed in some detail over the past several years and published largely in physics literature (Schimansky-Geier et al., 1995; Erdmann, 1997; Schweitzer et al., 1998; Ebeling et al., 1999; Erdmann et al., 2000; Schweitzer, 2003). The ABP theory is based on continuous motions in time and is described by a set of stochastic differential equations. A second approach has been developed, which is based on the random walk theory (called RWT from now on). It has been applied to particles that move in discrete “hops” with a pause at the end of each hop (Ordemann et al., 2003a,b,c). Though originally conceived without a self-propelling velocity (Schimansky-Geier et al., 1995), the present ABP theory deals with particles that are self-propelled and move through a dissipative medium, such as water. The particles expend energy in order to move and to supply their own metabolic requirements, while foraging for food represents an energy uptake.

These notions are conveniently expressed in terms of an effective, velocity dependent dissipation, $\gamma(v)$, which can assume positive and for small velocities possibly negative values. For $\gamma(v) < 0$, energy is pumped into the particle and may be stored in a depot (Ebeling et al., 1999) (there is more than sufficient food to supply the energies of motion and metabolism), while for $\gamma(v) > 0$ the rate of energy uptake and conversion is insufficient to maintain the supply in the depot causing the particle to slow down. The particle then finds a velocity for which, on average, the effective dissipation is zero, and this value is the self-propelling velocity. See Fig. 1 below. The right/left symmetry of these motions may be broken by parallelizing interactions, what could be any kind of a velocity aligning force. Single or groups of ABPs can move in a central potential which insures that they are confined to some region in space. Here we confine our model to a quadratic potential representing a linear restoring force. In addition, a random force, or noise, is applied in order to represent the variability inherent in a real animal’s motions. In contrast to the ABP theory, the RWT begins with the assumption of an average, constant self-propelling velocity, as does another approach (Vicsek et al., 1995). Each particle moves by hopping and turning. At the end of each hop a change in direction is taken from an experimentally measured turning angle distribution and a “kick” to-

* Corresponding author.

Email address: udo.erdmann@physik.hu-berlin.de (Udo Erdmann).

URL: <http://www.udoerdmann.de/> (Udo Erdmann).

ward a center of motion is applied. Random selections from the turning angle distribution represent the noise and the kick insures that the particles are confined. Here we take the kick to be a force linearly proportional to the distance between the particle and the center of the field. Both theories describe systems that operate far from thermodynamic equilibrium, since motion is maintained in the dissipative medium by a continual uptake of energy.

In the ABP theory, coherent motions at low density are modeled by interactions with the central field plus noise only. Two attractors motions are separated by a bifurcation controlled by the magnitude of the self-propelling velocity (Schweitzer et al., 1998): one a noisy fixed point and the other a pair of symmetric, limit cycles (recurrent closed paths) with equal probabilities to show a clockwise (CW) or counterclockwise (CCW) rotational sense in a plane (Erdmann et al., 2000). See Fig. 2 below. Other systems, for example molecular motors (Jülicher et al., 1997), which are also far from equilibrium and behave according to a similar velocity dependent dissipation, also show bimodal velocity distributions, that is, motion in two opposing directions that is equally probable (Badoual et al., 2002). The theory presented here is two-dimensional so that these motions are confined to the x - y plane. A particle-particle attractive interaction is then built in (Ebeling and Schweitzer, 2001; Erdmann et al., 2002a). The interaction is global in the sense that every particle feels the attraction of every other one but the strength decreases with pair separation distance. Such interactions result in a central mean field and predict swarming behavior, the gradual increase of particle density around the symmetry axis of the central field. Finally, a particle-particle hydrodynamic interaction is included that models the tendency for nearby particles (feeling one another's flow field) to align the directions of their velocities (Erdmann and Ebeling, 2003). This interaction breaks the symmetry of the two limit cycles leading to a collective vortex-type motion in one or the other rotational direction. A short range repulsive potential that results in avoidance when two particles come closer than some minimum distance can also be used to break the symmetry and lead to vortex formation. The sense of rotation of the vortex depends on an initial condition that is random, so that the final motion can be either CCW or CW.

Thus the ABP theory predicts four basic types of motion if the particles are confined: 1) noisy fixed point whereby a particle moves randomly about and through a single point in space; 2) two limit cycles whereby the particle moves on closed paths with CCW or CW directions equally probable. The second type can be separated again in two different types of motion if we investigate larger populations of interacting individuals: 3.1) swarming whereby initially randomly and widely dispersed particles first move toward a spatial center and then start rotating around this center (rotational motions in both directions are equally probable, and thus the net rotational motion is on average zero); and 3.2) vortex whereby all particles spontaneously align their velocities and

commence rotation in the same direction, because of a higher density of the individuals. As we show below, all four of these motions can be observed in laboratory experiments within a single species: the light sensitive zooplankton *Daphnia*.

Such motions, in addition to other collective behaviors, are commonly observed (Parrish and Edelstein-Keshet, 1999) in schools of fish (Weihs, 1973a,b; Hall et al., 1986; Parrish et al., 2002), bacterial colonies (Ben-Jacob et al., 1994), slime molds (Levine and Reynolds, 1991; Bonner, 1998; Dao et al., 2000) and flocks of birds (Larkin and Frase, 1988). Vortex motions were specifically observed long ago in colonies of ants by Schneirla (Aronson et al., 1972) and more recently in bacterial colonies (Czirók et al., 1996) and slime molds (Rappel et al., 1999). Swarming is of course quite well known. See for example (Okubo and Levin, 2001; Parrish et al., 2002). The idea of a self-propelling velocity arose early (Weihs, 1973b), and was expressed by Sakai whose model predicted the aforementioned four types of motion already in 1973. See a discussion on that early work in the useful book (Okubo and Levin, 2001). General reviews on the physics of individual particle motions and aggregation (swarming) has been given by Ben-Jacob et al. (2000) and Flierl et al. (1999). More recent theories, based on the idea of a self-propelling velocity, incorporated various couplings among the particles such as directional averaging of the vector velocities (Ben-Jacob et al., 1994; Vicsek et al., 1995; Levine et al., 2001; Couzin et al., 2002). A hydrodynamic generalization of these “rule based” theories was later developed by Toner and Tu (1995, 1998). In contrast to these, the ABP theory, based on the energy depot model (Ebeling et al., 1999), is represented by stochastic differential equations.

Our objective here is to summarize the ABP and RWT theories without burdening the reader with excessive detail and to compare the predictions of those theories at each step in their development with our experimental results on the motions of *Daphnia*.

2 Outline of the ABP Theory: single particle case

In 1827 the British botanist, Robert Brown, observed irregular motions of microscopic particles in water. He noted that their motions resembled that of living creatures. Later all such entities whose motions are mediated by random forces came to be called “Brownian Particles”. In a two-dimensional spatial plane, x - y , they are located by a vector \vec{r} , whose magnitude is $r = \sqrt{x^2 + y^2}$ and move with velocity, $\partial_t \vec{r} = \vec{v}$. Physical models represented by stochastic differential equations, called Langevin equations, describe the motion of these particles. They represent a balance of forces on the particle: the random force, or noise $\sqrt{2D}\xi(t)$, where D is the noise strength; the confining restoring force,

$\nabla U(r)$, where $U(r)$ is the external potential energy, the passive friction $-\gamma_0\vec{v}$ and, in our case, the self-propelling force $d e(t)\vec{v}$ that results from conversion of energy out of an internal energy depot $e(t)$ into motion;

$$m\partial_t\vec{v} = -\gamma_0\vec{v} + d e(t)\vec{v} - \nabla U(r) + \sqrt{2D}\vec{\xi}(t). \quad (1)$$

The noise, $\vec{\xi}(t)$, in this equation is external in the sense that it is contributed by the environment in which the particle finds itself. In the case of ABPs this noise could arise, for example, from thermal collisions, hydrodynamic fluctuations or turbulence. This noise is assumed to be “white”, that is its autocorrelation function is a delta function, $\langle \xi_i(t)\xi_j(s) \rangle = 2D\delta_{ij}\delta(t-s)$, Gaussian distributed and with zero mean. As an identifier, we will call this the “external” noise. Further, from now on we will choose units in which $m \equiv 1$. The time evolution of energy stored in the depot is given by $e(t)$, which is described by a second equation,

$$\partial_t e(t) = q_0 - c e(t) - d v^2 e(t), \quad (2)$$

that represents a balance among three processes: q_0 which is the energy inflow available to the depot, here called the uptake, for example from foraging for food; $-c e(t)$, which is a constant drain representing, for example, a metabolic requirement; and $d v^2 e(t)$, which is the power dissipated necessary to propel the particle through the medium. Here, c and d are constants. We take the available energy inflow q_0 , to be uniformly distributed over the two-dimensional space, though in more general treatments it can be irregularly distributed, $q(\vec{r})$ representing, for example, food availability in patches (Steuernagel et al., 1994; Schweitzer et al., 1998).

A key issue is the velocity dependent dissipation, $\gamma(v)$. Here we mention two different commonly used treatments. The first is the Rayleigh law, $\gamma(v) = -\gamma_1 + \gamma_2 v^2$, where the two γ 's are constants serving to delineate constant and velocity dependent contributions to the dissipation. After initial transients die out, the particle assumes a self-propelling velocity, $v_0^2 = \gamma_1/\gamma_2$. This law was originally developed to describe dissipative energy pumping in systems involving sound (Rayleigh, 1894) and has been used to describe self-propelling velocities applied to fish schooling (Niwa, 1994, 1996). The second is a law developed by Schienbein and Gruler (1993), $\gamma(v) = \gamma_0(1 - v_0/v)$, developed to describe the motions of various motile biological cells. The same friction law was used independently by Helbing and Molnár (1995) to describe the motion of pedestrians. Both of these laws have singularities, the former in a range of $v \gg v_0$, and the later for $v \rightarrow 0$. A key simplification can be obtained by assuming that the energy uptake rate $e(t)$ is slow compared with the dissipative rates. Equation (2) can then be adiabatically eliminated, $\partial_t e(t) = 0$, which, together with Eq. (1), results in a third dissipation law that does not suffer

from singularities and thus is more physically reasonable (Erdmann et al., 2000),

$$\gamma(v) = \gamma_0 - \frac{q_0 d}{c + dv^2}, \quad (3)$$

where γ_0 is the dissipation constant in the limit of high particle velocity. This function is shown in Fig. 1 where the velocity ranges of energy pumping into the depot (super-critical pumping) and dissipation from it (sub-critical pumping) are indicated separated by the self-propelling velocity at zero effective dissipation,

$$v_0^2 = \frac{q_0}{\gamma_0} - \frac{c}{d}. \quad (4)$$

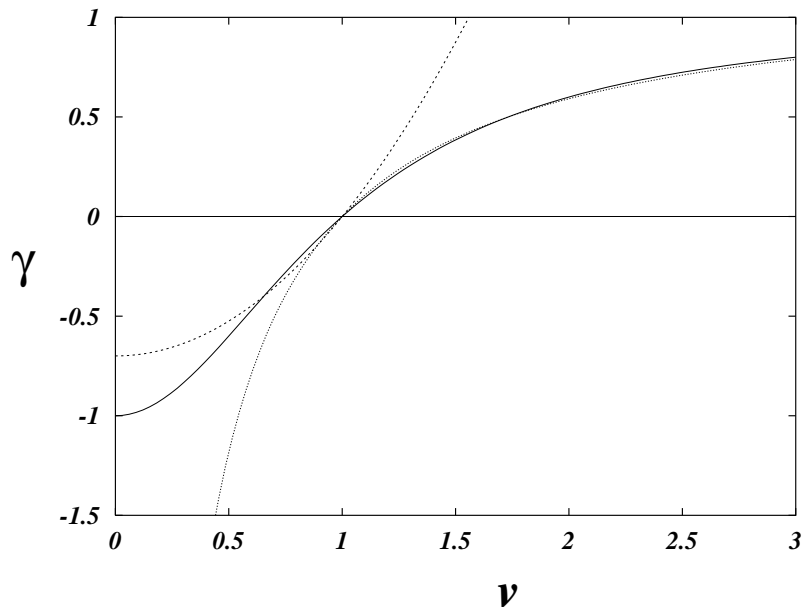


Fig. 1. The velocity dependent friction function, Eq. (3) showing sub- and super-critical energy pumping regions separated by the self-propelling velocity for which the effective dissipation is zero. The Rayleigh and Gruler formulae are shown by the dotted and dashed lines, respectively. The values of the parameters are, $q_0 = 10$, $c = 1.0$, $\gamma_0 = 2.0$, and $d = 0.7$

The solutions of Eq. (1) using the formula Eq. (3) give the first two types of motion separated by a bifurcation. The bifurcation parameter can be defined as the ratio of constants,

$$\mu = \frac{q_0 d}{c \gamma_0}. \quad (5)$$

Introducing a force $\nabla U(\vec{r}) = \omega_0^2 \vec{r}$, attraction by a light shaft, chemotaxis and similar causes can be modeled. For such a quadratic attractive potential (the force is linear in \vec{r}) two-dimensional motion with natural frequency ω_0 on closed paths in the x - y plane is possible. For $\mu < 1$, there is sub-critical pumping of energy and the motion is random around the symmetry point of the central potential, called here the “noisy fixed point”; and for $\mu > 1$ the pumping is super-critical, and the resulting motion is a symmetric pair of noisy limit cycles. Particles move on the limit cycles with the self-propelling velocity $|\vec{v}| > 0$. These limit cycles are closed curves in the x - y plane, and their symmetry represents the fact that the two senses of rotation, CCW and CW, occur with equal probability. This bifurcation is shown in Fig. 2, where the probability densities of the velocity components v_x and v_y are plotted showing the monomodal peak (noisy fixed point) in Fig. 2(a) for $\mu < 1$ and the bimodal density (limit cycles) in Fig. 2(b) for $\mu > 1$. The insets show example trajectories in the x - y plane.

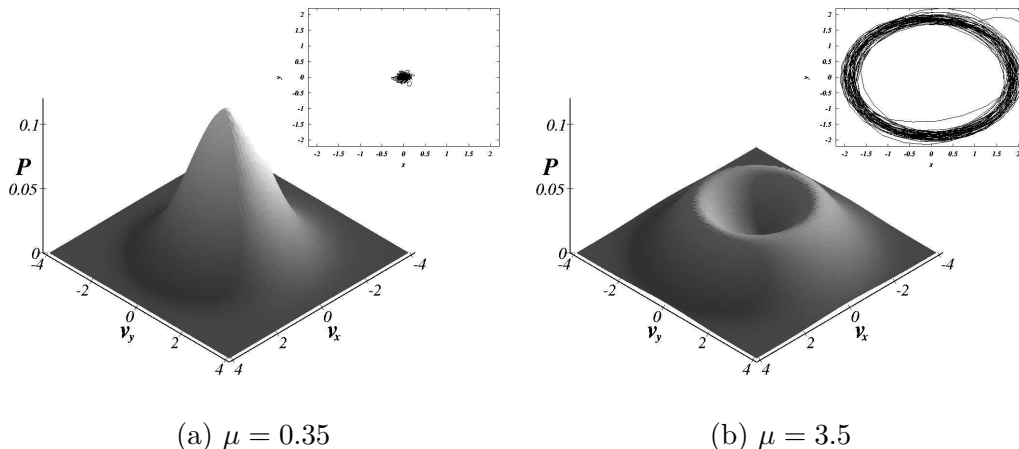


Fig. 2. The probability densities of velocity in the two-dimensional plane showing the noisy fixed point for $\mu = 0.35$ in (a) and the limit cycles for $\mu = 3.5$ in (b). The other parameters are $\gamma_0 = 2.0$, $D = 2.0$, $c = 1.0$ and $q_0 = 10$. The insets show typical trajectories in the plane

The foregoing theory applies to a single particle or to a collection of identical non-interacting particles moving at a unique self-propelling velocity in a attractive central potential. Below, however, we compare the theoretically predicted motions to those we actually measure for populations of *Daphnia*. In this case, the individuals are not identical. One way this population variability could be modeled is by building in a distribution of power conversion rates as given by the last term on the right in Eq. (2). In our populations, some *Daphnia* are young and presumably cannot convert energy at the same rate and thus cannot swim as fast as older individuals. We thus modify Eq. (3) by

allowing the strength of the power dissipated in motion to become noisy,

$$d \rightarrow d_0 + \eta(t), \quad (6)$$

where $\eta(t)$ is noise, which, in contrast to the external fluctuation, $\vec{\xi}(t)$, is an internal fluctuating variable within the population, meaning that different individuals have different values of d . We call this the population noise. It is Gaussian distributed with zero mean, has standard deviation σ_d , and is delta correlated (see also Erdmann et al. (2000), where a factor describing the efficiency of conversion is added to the model). This translates into a noisy dissipation as given by Eq. (3). Using Eqs. (1) and (3) with (6), we can obtain trajectories and measures directly comparable to the experimentally measured ones as we show in the next section below. Here we calculate the probability densities of velocity for two conditions of noise as shown in Fig. 3. The solid line represents density with the noise in Eq. (1) only (the external noise) and the dashed line represents both noises accounting for external and population variability. The net result of including population variability in the theory is

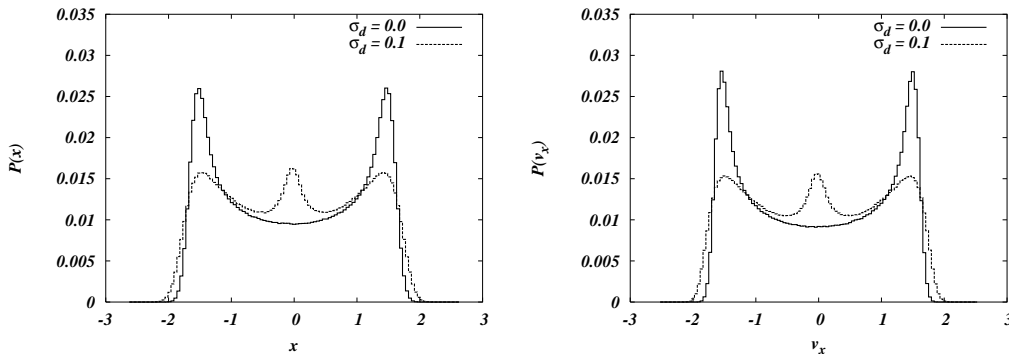


Fig. 3. The probability density of radii and velocities projected on the x -axis for the single noise $\vec{\xi}(t)$ in Eqs. (1) and (2) shown by the solid line, and for both noises, $\vec{\xi}(t)$ and $\eta(t)$, in Eqs. (1) and (6) shown by the dashed curve.

that there is now a distribution of both radii and velocity at which the particles travel, a quantity that can be directly measured in the experiment. Note that for some of the creatures the energy conversion is not efficient enough to reach the limit cycle. These participate in Brownian motion around the fixpoint (see inset of Fig. 2(a)). This is indicated by the maximum around zero in both graphs of Fig. 3.

3 About *Daphnia*

Daphnia are found in many species in fresh water over the entire globe. Figure 4 shows a single individual. They have a long evolutionary history and



Fig. 4. A single *Daphnia magna* with a store of eggs under the carapace. The two large antennae enable the animal to swim. An array of smaller appendages enables feeding. The animals range in size from about 3 to 5 mm in length.

consequently have developed a range of complex behaviors that insure their survival in various environments both stressed and nonstressed. *Daphnia* are known to heavily depend on phototaxis, for example when searching for food (Young and Getty, 1987), to confuse and avoid predators (Jensen et al., 1998) or for performing diel vertical migration (Zaret and Suffern, 1976; Rhode et al., 2001), a behavior whereby *Daphnia* swim near the water surface while feeding at night, but return to the depths during the day in order to avoid visual predators (most planktivore fish). They are strongly attracted to light in the visible range (VIS), repelled by ultraviolet (UV) and blind to infrared (IR), three facts that we will make use of in the experimental design outlined below.

It is not likely that *Daphnia* can form an image with their eyes according to Buchanan and Goldberg (1981). Unlike birds and fish, no direct visual alignment between *Daphnia* has been detected (Okubo and Levin, 2001). They can, however, determine wavelength, intensity, and direction of light (Smith and Macagno, 1990). *Daphnia* also use chemotaxis (Larsson and Dodson, 1993) and can detect water motions with their mechanoreceptors (Haury and Yamazaki, 1995). Because there is no known mechanism of long-range communication between *Daphnia* (Larsson and Dodson, 1993) in order to display coherent motions they must be individually attracted to a landmark such as a shaft of VIS light (Jensen et al., 1998). This can be easily demonstrated with a vertical flashlight beam in a dark aquarium as shown in Fig. 5. The swimming behavior of *Daphnia* is dominated by the fact that they live in a relatively low Reynolds number environment (Zaret, 1980). They move with an average ‘hopping’ rate of approximately three moves per second and their overall speed is 4-16 mm/s with a sinking rate of approximately 3 mm/s (Dodson, 1996). See an example 3-dimensional trajectory in Fig. 6. *Daphnia* at low density (about one individual per liter), swimming in the dark, do not show evidence of any long-range interactions. (There is, however, a short-range repulsion leading to avoidance



Fig. 5. *Daphnia* are attracted to VIS light as shown by this vertical flashlight beam. Three side view snapshots taken at 20 second intervals show the gathering of *Daphnia* (white dots) in the shaft of light.

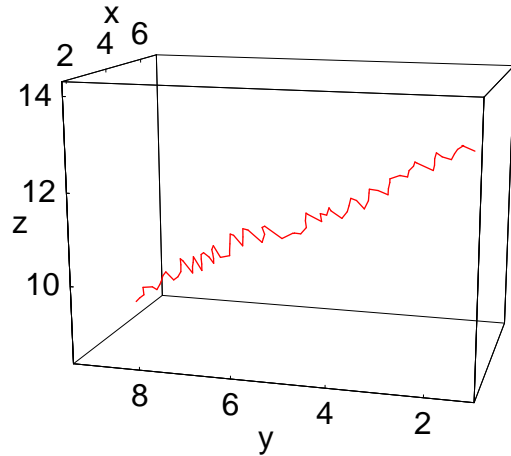


Fig. 6. Typical trajectory measured on a *Daphnia* in darkness in three dimensions. This trajectory illustrates the hop and sink motion with a change of direction between successive hops.

maneuvers during close encounters.) Therefore, their motion can be modeled by the ABP theory of single self-propelled particles moving in a central field and subject to noise.

4 Experiments with small *Daphnia* density

The apparatus designed to investigate the aforementioned motions is shown in Fig. 7. It consists of a rectangular aquarium (50×20 cm, water level 25cm) with a vertical translucent plastic tube (30 cm long by 1 cm diameter) mounted in the center. The tube is illuminated with VIS light from above by a fiber optic cable thus forming a shaft of light propagating radially outward. This forms a vertical marker with cylindrical symmetry to which the *Daphnia* are attracted. A filter to remove IR from the light shaft is placed between the illuminator and the fiber optic cable. *Daphnia* within the aquarium are illuminated by IR from arrays of filtered IR-Light Emitting Diodes located on either side as shown. IR sensitive video cameras (Baxall, Cohu) fronted by filters to remove

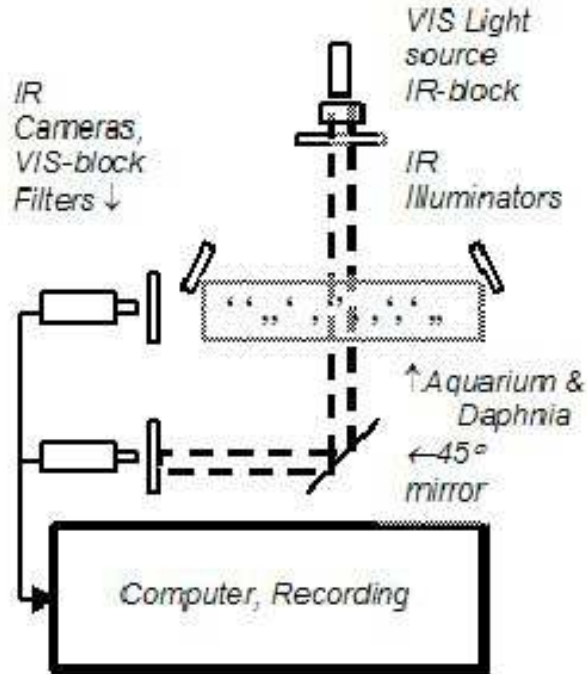


Fig. 7. The apparatus, showing the light source and cylindrical VIS light shaft, the IR illuminators and cameras. *Daphnia* motions can be observed and recorded simultaneously in side and bottom views. Appropriate filters are arranged such that *Daphnia* are recorded in IR while responding to and seeing only VIS.

VIS light obtain side and bottom views of the aquarium. The bottom view is afforded by a 45° first surface mirror. Images from the cameras are combined on a split screen viewer, recorded simultaneously on magnetic tapes, then later digitized and saved on large capacity disks in a PC. The trajectories are analyzed with the tracking software (Chromotrack® Version 4.02 from San Diego Instruments, or TrackIt from IguanaGurus). In a later improvement, the video cameras were replaced by an IR capable camcorder (Sony DCRTRV80) with filters to block VIS. With this arrangement digital data can be streamed directly to the computer.

After placing 20 to 80 *Daphnia* in the water with algae (*Scenedesmus quadricula*) for food and leaving them to acclimate and to distribute uniformly for at least 15min, the VIS light shaft is switched on. Being individually attracted to the optical marker, a substantial number can be observed to move on circular paths around the light shaft in both directions (CW and CCW) with frequent reversals of direction. The radii of their tracks are large enough (typically 1 to 5 cm) to exclude the possibility that this behavior occurs simply due to the hydrodynamic sensing of an artificial object presumably with their mechanoreceptors. Experiments show that *Daphnia* can sense static objects at distances not exceeding about one to two body lengths (Haury and Yamazaki, 1995). Similar circling behavior was observed in the absence of any solid object in more recent experiments using a high intensity flashlight shining vertically

into the water instead of the solid light tube (Nihongi et al., 2003). Typical tracks are shown in Fig. 8(a) for about 40 individuals and Fig. 8(b) for a single individual that makes seven complete CCW turns and a reversal of direction around the central marker. Arrows indicate the rotational directions. The trajectories look as in the theory shown in the inset of Fig. 2(b). While these

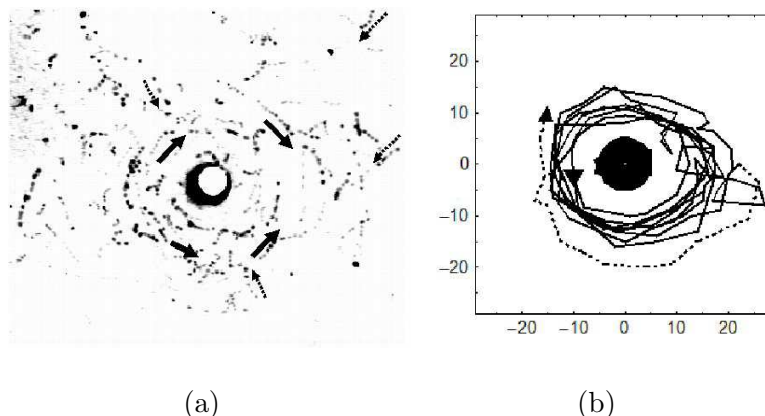


Fig. 8. Bottom view of individual *Daphnia* motions around the light shaft. (a) About 40 distinguishable individuals, visible as a chain of five black dots for each animal, (grey scale inverted for easier recognition, time interval between single dots 0.3 sec) are engaged in circular motions indicated by filled arrows with approximately equal numbers traveling CCW and CW. The 1 cm diam. white circle is the end view of the light shaft with VIS light blocked. The dashed arrows in the outer areas of the field of view indicate *Daphnia* that are moving towards the light. (b) The track of a single individual making seven CCW turns (solid line, start marked by arrow) around the light shaft and showing a reversal toward the end of the track (dashed line, end marked by arrow, coordinates in mm).

results from experiment and theory seem quite similar, statistical measures are necessary for quantitative comparisons.

An essential point is that single *Daphnia* make rotational motions around the central attractant. This indicates that, for *Daphnia* at least, circling is not an emergent or self-organized motion that occurs as an inherent property of a swarm of animals (Parrish and Edelstein-Keshet, 1999). Circular motions in zooplankton at low density were observed previously (Young and Getty, 1987; Young and Taylor, 1990) but only incidentally in the course of different experiments. Below we show that high-density swarms of *Daphnia* are capable of vortex motions similar to those observed in bacteria (Czirók et al., 1996), slime molds (Rappel et al., 1999) and fish (Parrish et al., 2002). But in *Daphnia* the onset of the vortex is the result of a symmetry-breaking process that transforms the two symmetric limit cycle motions (CCW and CW), observable for single individuals in both theory and experiment, into motion in one direction only. Certainly individual birds in some cases follow rotational paths around central attractive markers (Larkin and Frase, 1988). Possibly bacte-

ria and fish do also. It is therefore not demonstrated that the vortex motion sometimes observed in swarms of these animals is an “emergent” property unrelated to the motions of individuals.

We turn now to statistical measures of *Daphnia* motions at small density. The dominant part of the motion of single *Daphnia* in the light field takes place in the horizontal plane. Indeed individuals tend to circle in layers with little vertical migration, as we have observed in 3-dimensional tracks obtained in the laboratory of J. R. Strickler. To restrict the characterization of motions, analyzing only the bottom-most layer, we measure the amount of circling, we measure the heading angles for several *Daphnia*. The heading angle, θ , is defined as the angle between a single hop and the direction to the light shaft as shown in Fig. 9(a). This di-

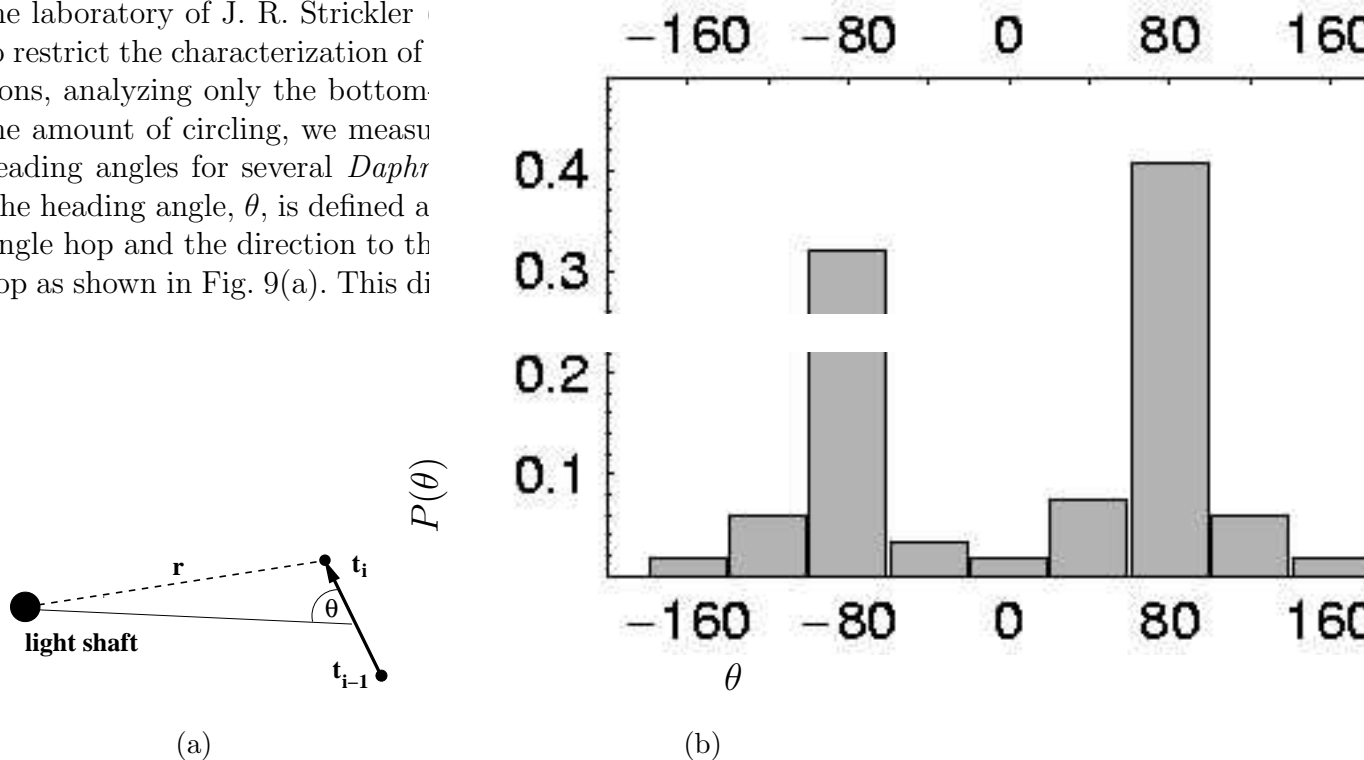


Fig. 9. The heading angle. (a) Definition of the heading angle, θ , as measured for every hop movement of an individual. (b) Histogram of heading angles, $P(\theta)$, obtained from 624 hops from the tracks of four individuals. Plot (b) is adapted from Ordemann et al. (2003b).

cated at approximately $\pm 90^\circ$. It indicates two properties of the motion: First, the twin peaks at $\pm 90^\circ$ demonstrate that the average motion is resolved into two rotational directions, CW ($+90^\circ$) and CCW (-90°). Second, the magnitudes of the two peaks are nearly equal, demonstrating that the CW ($+90^\circ$) and CCW (-90°) motions occur with approximately equal probabilities. Both of these experimental observations are predicted by the ABP theory.

For the same set of hops we obtained a histogram representing the probability distribution $P(r)$ of the distance r of the *Daphnia* to the light shaft as shown in Fig. 10(a). Figure 10(b) shows a histogram of the angular momentum, again with twin peaks of approximately equal magnitudes. In Fig. 10(c) we show a histogram of the average length of circling in one direction (CW or CCW)

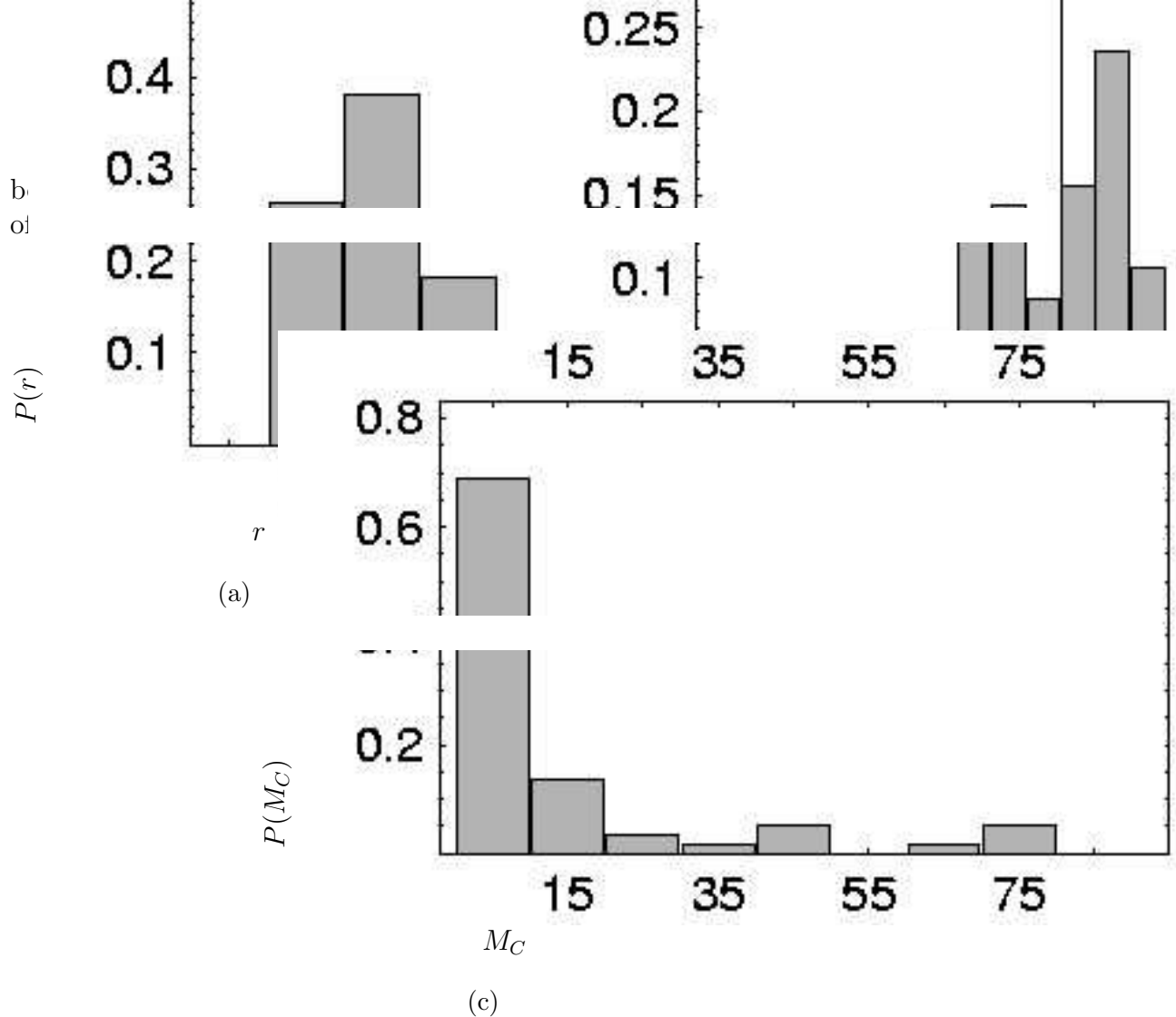


Fig. 10. Histograms of (a) the circling radii, $P(r)$, (b) the angular momentum, $P(L_{\text{ang}})$, and (c) the directional reversals, $P(M_C)$. These data were obtained from the same set of hops using the same track data as for Fig. 9. Plots are adapted from Ordemann et al. (2003b,c).

5 The Many Particle ABP Theory

When there are many particles with a long range attractive interaction between them, the global effect is that the particle-particle interactions can be replaced by a mean field. This field is the result of a central potential that causes confinement of the particles. This phenomenon can actually be demonstrated in experiments with the zooplankton *Chydoridae*. A long range attractive interaction can be switched on by causing one or a very few individuals to become visible to all the others by shining light on them. When that happens all animals are attracted to the visible few. The light scattered from the few must, however, dominate the visual environment. This demonstration has been realized in the laboratory of J. R. Strickler by directing a narrow, blue, VIS,

laser beam vertically into an aquarium which, apart from the beam, is dark. The beam itself cannot be seen by the animals in the tank since the medium is clear and the beam is very narrow. Many animals are initially distributed either at the bottom or throughout the aquarium. One or a few individuals by accident swim into the beam, become brightly illuminated, and thus become visible to all the rest. The remaining individuals are attracted by this light, immediately begin migrating toward the beam and become illuminated themselves, thereby intensifying the attraction, a positive feedback effect whose strength is dependent on the number illuminated (see Fig. 11 in Strickler (1998) and the movie at http://www.uwm.edu/~jrs/out_of_corners.htm). Thus the motion mimics that of a large number of animals in a central attractive potential, but in this case arises solely due to a long range, indirect attractive interaction between the animals. Zooplankton in the dark, or in the aforementioned aquarium without a single individual in the beam to scatter light, show no evidence of a direct long range interaction.

In the theory we can add the attractive interaction summed over all particles and this will enter an equation of motion similar to Eq. (1) but now representing the balance of forces on one of the particles, i , in the ensemble,

$$m\partial_t\vec{v}_i = -\gamma_0\vec{v}_i + d e_i(t)\vec{v}_i - \kappa_h \left[\vec{r}_i - \frac{1}{N} \sum_j \vec{r}_j \right] + \sqrt{2D}\vec{\xi}_i(t), \quad (7)$$

and the energy uptake of the i -th particle is,

$$\partial_t e_i(t) = q_0 - c e_i(t) - d v_i^2 e_i(t). \quad (8)$$

Equations (3) and (4) remain the same except that the velocity must be indexed: Moreover, if we build in the effect of population variability, then the parameter, $d \rightarrow d_i$ in Eqs. (3)–(5), where the population noise in Eq. (6) results in a Gaussian distribution of the d_i . Notice that in Eq. (7) the term in square brackets has replaced the force generated by external potential $-\nabla U(\vec{r})$. Moreover, the force is linear in the distance between particles, $\vec{r}_i - \vec{r}_j$, so that the mean field potential is quadratic as before, and its strength is adjusted with the coupling constant κ_h .

The many-particle theory as outlined here, leads to results similar to those predicted by Eqs. (3)–(5), in particular, there is a bifurcation from a noisy fixed point motion to the symmetric pair of limit cycles except now the entire population participates in these motions. For simplicity, we treat this problem only considering the environmental noise, $\vec{\xi}(t)$, appearing in Eq. (1), though in the many particle case, Eq. (7), an independent noise, $\vec{\xi}_i(t)$, applies to each particle in the population. The appropriate measures are thus probability densities in both coordinate and velocity space. In addition to these motions, the

theory predicts the third motion of our suite: swarming. A large population of particles, initially widely and randomly dispersed, as shown in Fig. 11(a), begin to migrate toward the center of mass of the colony when the inter-particle interactions are switched on as shown in Fig. 11(b). Their individual motions are largely rotational, but this is not visible to the eye, since on average equal numbers rotate in opposite directions. The CW and CCW motions are marked by arrows in the Figure. Figure 11 shows example trajectories but the appropriate measures are probability distributions of spatial and velocity coordinates on the x - y plane.

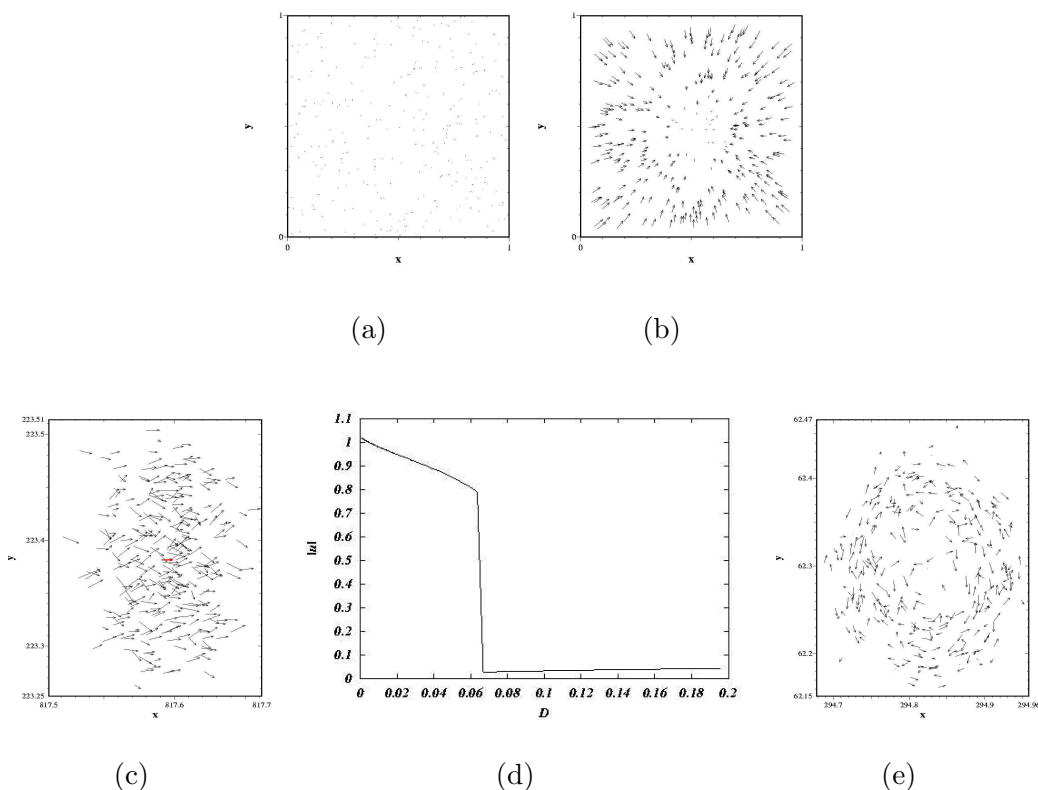


Fig. 11. Swarming in the many particle ABP theory. (a) Initially many particles are widely dispersed to random positions. (b) Under the influence of their mean field, they move toward the center of mass. (c) Directed motion. (d) Noise induced collapse of translational velocity to zero mean translation for $D > D_{\text{crit}}$. (e) Both sets of initial conditions finally converge on an equilibrium state is established with approximately equal numbers of particles rotating CW and CCW. The mean radius of the two limit cycle distributions depends on the mean self-propelling velocity.

The simulations of the many particle theory show another interesting phenomenon that is observable for a different set of initial conditions as shown in Fig. 11(c). The particles are still initially randomly distributed over the plane, but now each is given the self-propelling velocity and all vectors are initially parallel (in this case pointed in the x direction). We call this directed motion.

For noise intensity smaller than some critical value, $D < D_{\text{crit}}$, the particles continue to move with a mean translational velocity, but for $D > D_{\text{crit}}$, the mean translational velocity rapidly descends to zero and the motion is all rotational (again with equal probability for CW and CCW motions). This is a new type of noise induced transition (see e.g. Horsthemke and Lefever, 1984) and it is shown in Fig. 11(d). The critical noise intensity, D_{crit} , depends on the parameters of the velocity dependent dissipation, $\gamma(v)$, and has been calculated in the limit of large population density (Erdmann et al., 2002b). For both sets of initial conditions, the final state is the set of two symmetric counter-rotating limit cycles, as shown by the example trajectories in Fig. 11(e).

6 Experiments with large *Daphnia* density

Swarms are often formed for different purposes, such as enhanced feeding, mating and offspring rearing, by self-propelled animals living and moving in three-dimensional environments. Besides this, many animals are thought to form swarms to confuse and avoid predators (Humphries and Driver, 1967; Hamilton, 1971; Pulliam, 1973, see also Parrish and Edelstein-Keshet, 1999 and Okubo and Levin, 2001). Swarming for this purpose seems common to a number of animals including planktivore fish, for example, sardines, mackerel and anchovetta (Partridge, 1982; Hall et al., 1986), zooplankton (Jakobsen et al., 1994; Kvam and Kleiven, 1995) and some species of birds (Caraco et al., 1980). Such swarms, occasionally also associated with rotational motions, have been called self-organized or emergent structures (see e.g. Parrish and Edelstein-Keshet, 1999; Camazine et al., 2001; Okubo and Levin, 2001) meaning that there is no single leader nor a dynamical process that governs the motions of individual animals in such a way as to give rise to the swarm structure.

We can consider swarming to be simply a local increase in density of animals without a net global coherent motion. An attractant, such as a light marker is usually necessary (e.g. Jakobsen and Johnsen, 1988; Buskey et al., 1996). An additional collective motion, however, has been observed in swarms. According to anecdotal evidence, transitions from more-or-less random motions to an average, coherent rotational motion have sometimes been observed in the field. These are called vortex motions and have actually been described in detail for a species of oceanic plankton (Lobel and Randall, 1986). In the laboratory, vortex motions have been studied in bacterial colonies (Ben-Jacob et al., 1994; Czirók et al., 1996) and slime molds (Rappel et al., 1999) but have not been well investigated for the larger animals largely due to limitations imposed by the size of the swarms, for example of birds and fish. The physical, biological, and chemical reasons for vortex-swarming are, consequently, not well understood. But the theories discussed here can provide at least a minimal set of conditions necessary for vortex formation. The symmetry of the pair

of limit cycles must be broken in order for the vortex to form. Symmetry-breaking processes based on pair avoidance (arising for example from short range repulsive potentials) are discussed in Sect. 7 below. In Sect. 8, we also consider hydrodynamic feedback as a symmetry breaking mechanism.

We have observed transitions to vortex motions in *Daphnia* swarms using the apparatus shown in Fig. 7 as well as in a cylindrical aquarium (about 50cm diameter) recorded with a digital camera from above. The vertical visible light shaft, provided either by a flashlight beam or by the cylinder of Lucite, is the central attractant. First, *Daphnia* are conditioned in the dark for typically 15 minutes in order that they assume an approximately random distribution. Then the light shaft is switched on. The following motions are typically observed. During the first few seconds, the animals swarm toward the light shaft as shown in Fig. 12(a). During this period no rotational motions can be observed; the animals simply rush toward the attractant. In the next period rotational motion becomes evident but with approximately equal numbers of individuals traveling in both directions (see Fig. 12(b)). Finally the individuals tend to align their velocities, and global rotational motion either in the CW or CCW direction occurs as shown in Fig. 12(c). We have observed that the

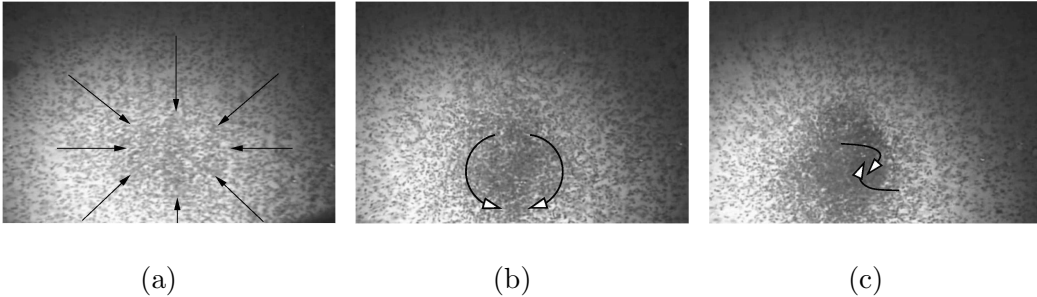


Fig. 12. Three top view snapshots taken at 5 second intervals show the formation of a *Daphnia* vortex-swarm. (a) *Daphnia* gathering at the light shaft, taken 5 seconds after switching on the visible light, (b) rotational motion of swarming *Daphnia* in both directions, CCW and CW, and (c) vortex-swarming in CW direction.

times for these processes to take place strongly depend upon the *Daphnia* density, being shorter for larger densities. Using some inert particles to decorate the water motion, we have noted that not only do the animals move but also the water moves in the same direction after the vortex is fully formed. Thus we call this a biological-hydrodynamic vortex. Below in Sect. 8, we describe this phenomenon as a physical phase transition. Within the framework of the RWT, we hypothesize that the symmetry of the limit cycle pair is broken by a positive feedback represented by a non-zero order parameter that evolves in time. If a momentary fluctuation results in even a small majority of animals circling in one direction with water being dragged along with them, then that direction becomes dominant as the other animals feel the hydrodynamic flow. Animals initially moving counter to the dominant flow then change their

direction thus forming the vortex.

In Section 7 below, we show that in order for the vortex to form, some symmetry breaking mechanism must be present. We suggest three possible processes: short range repulsion, avoidance and velocity aligning hydrodynamic coupling. *Daphnia* do exhibit avoidance events as discussed below in Sect. 7. It is important to understand that avoidance is different from collisions between particles mediated by a symmetric short-range repulsive potential.

7 How is the symmetry broken?

As discussed above, the two motions characteristic of small density experiments with *Daphnia*, and described by the theory for non-interacting particles, are the noisy fixed point followed by a bifurcation to a pair of closed paths (limit cycles) that describe the equally probable CCW and CW rotational motions in a central potential. Many particles with attractive interactions can exhibit the third motion - swarming - this is represented by collective motions toward a center together with the aforementioned bi-directional rotations. The fourth motion - the vortex - is also a many-particle phenomenon but is characterized by the single rotational motion of all the particles, and in the experiment, includes also fluid rotation. As we have seen, all these motions are observable in our apparatus, the former two with low *Daphnia* density and the latter two only in experiments with large densities. We also have mentioned that theoretically some symmetry breaking process is necessary in order to replace the two counter rotating limit cycles with a single vortex rotating in a single direction. The question is, in natural phenomena involving swimming animals, what is the symmetry breaking force or process?

We put forth two possibilities: short range repulsion and hydrodynamic self-alignment of velocities. Perhaps the simplest theoretical symmetry-breaking mechanism is offered by a symmetric short-range repulsive potential between pairs of particles. The physical laws governing scattering thus describe encounters among such particles. Avoidance is, however, not the same as particle scattering. It involves animate behavior and arises, for example, in dynamical descriptions of pedestrian avoidance maneuvers. Hydrodynamic coupling involves the overlap of the flow field due to the motion of one moving particle with that of another. As we show below, this coupling tends to align velocities leading to a final rotational state in one direction.

A third mechanism for symmetry breaking is collision avoidance. The first and second are discussed below in some detail, while this is only outlined as it has been described elsewhere. As we use the term here, avoidance has behavioral implications and thus involves mechanisms that cannot be described by

simple, symmetric potentials (Mach et al., 2003) as, for example, the Morse potential used below. We do not discuss avoidance in detail here. A similar problem arises in dynamical descriptions of pedestrian avoidance maneuvers (Helbing et al., 1994). These again lead to a symmetry breaking and consequently to various collective motions including the vortex formations of interest here.

Both scattering due to a symmetric short-range repulsive potential and hydrodynamic velocity alignment work equally well within the framework of the ABP theory to break the limit cycle symmetry. Unfortunately, at present the experiment does not provide enough information to distinguish between them. Moreover, Fig. 13, showing an actual encounter of two *Daphnia*, suggests that they execute a collision avoidance maneuver. Here two *Daphnia* are approach-

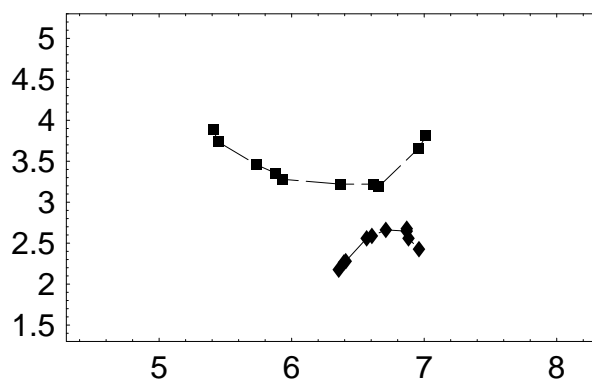


Fig. 13. Track of a bottom view of an example avoidance event. The two *Daphnia* are shown in their initial positions, being at the same height in the water column (as only a 6mm thick horizontal layer is illuminated by an IR laser and line generator). The tracking software is used to depict their trajectories through subsequent frames. In this example the *Daphnia* avoid each other, in a few other (rare) examples they actually collide.

ing each other in the horizontal plane, avoid each other and depart on different trajectories. Though we have observed numerous encounters between pairs of *Daphnia*, unfortunately, the detailed statistics necessary for realistic modeling have not yet been compiled.

7.1 Short-range repulsion

Let us assume that the interaction between the particles shows long-range attractive together with short-range repulsive behavior. As suggested by similarities to interactions between molecules, we use the Morse-potential to model this type of interaction. The resulting collective effect is the formation of clusters, a well known effect from solid state physics (Morse and Stueckelberg, 1929; Morse, 1929; Kittel, 1995). In the limit of large inter-particle separa-

tion, the Morse potential becomes approximately quadratic, that is, similar to the external and mean field potentials used in Sections 2 and 5. As those sections show, the self-propelling velocity together with a quadratic potential lead to rotational motions (the two symmetric limit cycles). But now, the short-range parts of the Morse potential parallelizes the neighbors and breaks the symmetry of the limit cycles, leading to rotation of the entire cluster in one (or the other) direction. As we know from the previous sections rotations are stable within such potentials. Thus we can think of a cluster with an initial condition such that all stationary velocities of the particles are equal in magnitude and additionally all have the same direction. Increasing the noise within the system leads to a phase transition as shown in Fig. 14, where, for D greater than a critical value, D_{crit} , the cluster stops its directed motion. The net motion of the cluster vanishes. Finally, this can lead to a rotation of the cluster. In this new type of noise-induced phase transition the

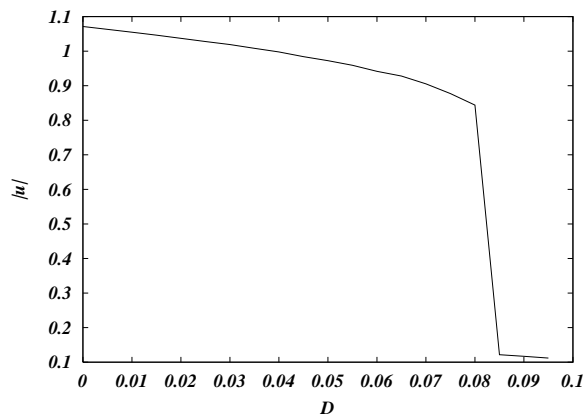


Fig. 14. Noise induced transition from directed to motion with zero mean translational velocity but non zero mean angular momentum (short range repulsive potential – Morse potential).

mean translational velocity crashes to zero for $D \rightarrow D_{\text{crit}}$ and is replaced by a mean rotational velocity. The stability of the rotational motions was discussed in detail in Erdmann et al. (2002a) and the noise-induced transition in Erdmann et al. (2002b).

7.2 Hydrodynamics in the ABP theory

Daphnia live in a low Reynolds number fluid environment. Hence, we can imagine that laminar flows of water mediate the interaction between individuals. The approach to use hydrodynamic interaction terms to model this coupling has already been used before for some species (Weihs, 1973a; Huth and Wissel, 1990; Niwa, 1994, 1996). With this in mind, we consider the dipole-like flow around one particle, j , that is moving at the self-propelling velocity. We want

to know the flow field of j at a distance r_{ij} at the location of particle i , as shown in Fig. 15. Considering similar contributions from all the other particles, a net hydrodynamic velocity v_F is present at the location i .

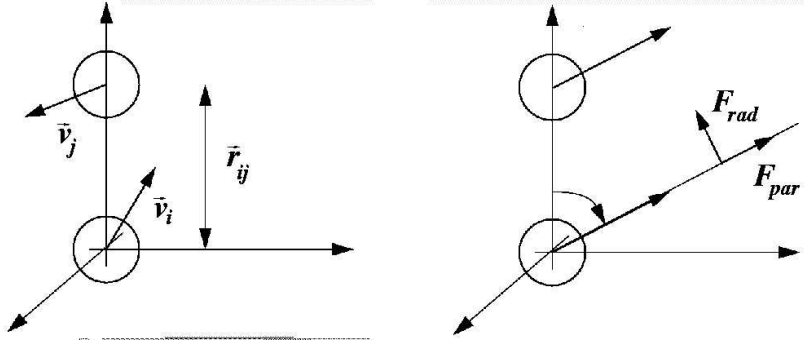


Fig. 15. Geometry of the hydrodynamic coupling showing parallel and perpendicular velocity components of the animals, before coupling through the flow field (left) and after coupling (right). $\vec{F} = \kappa_F \vec{v}_F$, where the vector velocities are defined in Eqs. (11)

In order to add a hydrodynamic interaction into Eq. (1), this stochastic equation of motion can be rewritten in the following way:

$$m \partial_t \vec{v}_i = -\gamma(v_i) \vec{v}_i + \kappa_F \vec{v}_F - \nabla U(\vec{r}_i) + \sqrt{2D} \vec{\xi}_i(t), \quad (9)$$

where the term $\kappa_F \vec{v}_F$ is generated by all the other moving particles, and the parameter, κ_F measures the strength of the hydrodynamic interaction. This term tends to align the direction of the velocity \vec{v} with that of \vec{v}_F . Thus particle i is finally dragged in the direction of motion of j . The aligning force, given by the new term in Eq. (9), originates with the viscosity of the surrounding liquid, and can be modeled by a well-known term in the Navier-Stokes equation (see e.g. Landau and Lifschitz, 1987). Within the laminar regime, and for low Reynolds number, the flow can be modeled by additive Oseen-contributions (Oseen, 1915a,b,c). This way of modeling hydrodynamic interactions is similar to the one used in the theory of electrolytes (Falkenhagen, 1971) and macromolecules (Hubbard and Douglas, 1993; Timoshenko and Dawson, 1995; Neelov et al., 2002). Within this approximation the flow field becomes

$$\vec{v}_F(\vec{r}_i) = \sum_{j \neq i} \frac{R}{r_{ij}} \left[\delta + \frac{\vec{r}_{ij} \otimes \vec{r}_{ij}}{r_{ij}^2} \right] \vec{v}_j \quad \text{valid for } r_{ij} \gg R, \quad (10)$$

where R is an effective hydrodynamic radius of the particles, and \otimes is a tensor product. Strictly speaking the Oseen-law is valid only asymptotically for $r_{ij} \gg R$. We do not claim that this is the only way to introduce hydrodynamic interactions, nevertheless the Oseen-law has the right symmetry properties.

This is to be seen from the alternative way of writing Eq. (10):

$$\vec{v}_F(\vec{r}_i) = \sum_{j \neq i} \left[\frac{R}{r_{ij}} \vec{v}_j + \frac{R(\vec{r}_{ij} \cdot \vec{v}_j)}{r_{ij}^3} \vec{r}_{ij} \right] \quad \text{valid for } r_{ij} \gg R. \quad (11)$$

This shows that the Oseen-flow consists of parallel and radial components. The first term on the right of Eq. (11) is the component of the flow field parallel to velocity of the particle i , and it is this component that tends to align velocities of i and j . The second term is the radial component and tends to act along the direction of the line of sight between i and j . The alignment effect that results in symmetry breaking and thus large-scale coherent motions is due to the parallel components.

If one imagines that we start with a population of active particles in a liquid medium, confined by a quadratic potential, due to the combination of active friction and external confinement on average half of the particles will rotate CW and the other half CCW. In contrast to particles that move in a vacuum, coupling is mediated through the liquid. This leads to an interaction as described, for example, by Eq. (11). Because the hydrodynamic interaction aligns the velocity vectors of the individuals the dual rotational motion breaks down and the final motion is of the entire population rotating in one direction. This direction is determined by random initial conditions. Additional motions, including clustering, global rotation of clusters and final rotational direction selection, result from this hydrodynamic interaction. These have been described in detail in (Erdmann and Ebeling, 2003).

8 Random Walk Theory (RWT)

8.1 Introduction

Discrete Random Walk Theories (RWTs) have been used extensively in biology, mainly to describe the irregular motions of bacteria (Berg, 1993). RWTs are iterative, that is a certain set of rules is applied to a particle located at a certain point in space in order to compute its future location and this process is repeated (iterated) to compute sets of jumps to successive locations. Since *Daphnia* naturally move in sequences of hops separated by pauses with a new direction of motion chosen at the end of each hop (see Fig. 6), RWTs can generate descriptive models of their motions. In this section we describe such a model and compare its predictions with experimental data. The experimental results reported in Section 4 for *Daphnia* at low densities indicate that the dominant interaction is with the central attractant and that inter-

animal interactions are much less important for low animal densities. Consequently theoretical models of self-propelled, interacting animals and their variants (Vicsek et al., 1995; Levine et al., 2001; Couzin et al., 2002) are not applicable to experiments at low densities with our animals. Though the ABP theory outlined in Section 2 adequately explains the noisy fixed point and limit cycle motions, we outline here a theory based on random walks. This theory has the advantage of being simple and easily simulated numerically, since it is only necessary to iterate and update an algorithm rather than to integrate a set of stochastic differential equations.

Any theory of *Daphnia* motion at low densities within an attracting field must predict the two observed motions: noisy movements near and through a fixed point and the rotational motions about the attractant. An obvious question arises: what are the minimum ingredients necessary to describe these motions? To answer this question, and to simulate the observed behavior of single *Daphnia*, we developed a self-propelled particle model based on random walks with the aim of being as simple as possible. The final model for low animal densities, closely related to the ABP theory, consists of only two ingredients: a short-range temporal correlation to simulate the general movement of the *Daphnia* in darkness and an attraction to the light marker (Ordemann et al., 2003b).

8.2 The Turning Angle Distribution

Discrete random walk models having memory, or correlation, are powerful tools to simulate various biological, chemical and physical processes that are more complex than pure Brownian motion (Hughes, 1995). In the case of our *Daphnia*, a short-range correlation is indicated by the fact that the animal's choice of turning angle, α , at the end of each hop is not completely random but instead is correlated to some degree with the previous direction. We have observed a large number of hops of *Daphnia* swimming in the dark. From these data we have assembled the distribution $P(\alpha)$ of turning angles (DTA), which turns out to be a bimodal symmetric distribution with a pair of maxima at approximately $\pm 35^\circ$ (Ordemann et al., 2003b). Shown in Fig. 16 is the distribution $P(|\alpha|)$ of the absolute turning angles, which resembles the results found for the DTA of the oceanic zooplankton copepod (Schmitt and Seuront, 2001). The presence of these maxima signals the existence of a short-range temporal correlation. If the directions of motion were completely uncorrelated, as for purely Brownian walkers, the DTA would be uniform. Thus *Daphnia* prefer moving in the forward direction and the most probable turning angles $\alpha_{\max} \cong \pm 35^\circ$ may have evolved to optimize the amount of territory covered while foraging in patchy food distributions (Gerritson and Strickler, 1977).

In constructing our RWT we introduce the random process (noise) by ran-

domly choosing a DTA shown in Fig

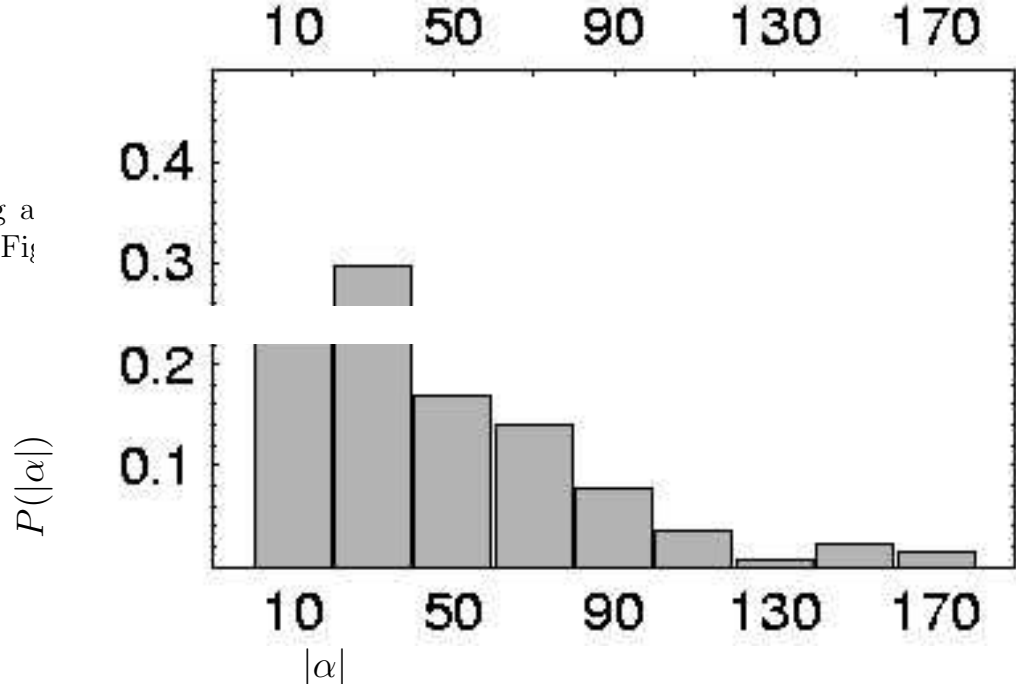


Fig. 16. The experimentally measured distribution of absolute turning angles, $|\alpha|$. The histogram was assembled from analysis of 1599 hops taken from eight animals moving freely in a dark aquarium with uniformly distributed food. The *Daphnia* were conditioned in the dark for a minimum of 15 min. before recording data. The turning angles were projected onto the two-dimensional horizontal plane. Plot adapted from Ordemann et al. (2003b).

correlation of only one iteration (time step). Though *Daphnia* may have a memory extending over a few hops, our observations indicate that this does not dominate the motion as the first hop memory does. Moreover, including only a one step memory keeps the model simple, which is our major aim. The particle in our RWT hops a fixed distance, Δx , in a time step, Δt , upon each iteration. Thus the magnitude of its velocity is a constant, and this is the self-propelling velocity. These model conditions are realistic, since the hop length and mean velocity of *Daphnia* are observed to be approximately constant (Dodson, 1996).

8.3 Motions Stimulated by Light

In order to simulate the behavior of *Daphnia* in a light field an attraction to the marker must be built into the theory. The ABP theory detailed above models the attraction with a linear restoring force in the direction of the center of motion. Similarly, we construct a "kick" proportional to the distance, r , of the particle to the light source and proportional to a normalized strength parameter $L/(1-L)$, where $[0 \leq L < 1]$. For every time step, the walker randomly chooses a directional change, α , from the DTA, then the kick, $[L/(1-L)]r$ towards the light is applied resulting in a new heading angle θ . The final heading vector, labeled $t_{i+1} - t_i$, is rescaled to unit length to maintain constant velocity of the walker. The geometry of a pair of iterations for the time steps $\Delta t = t_i - t_{i-1}$ and $\Delta t = t_{i+1} - t_i$ is shown in Fig. 17.

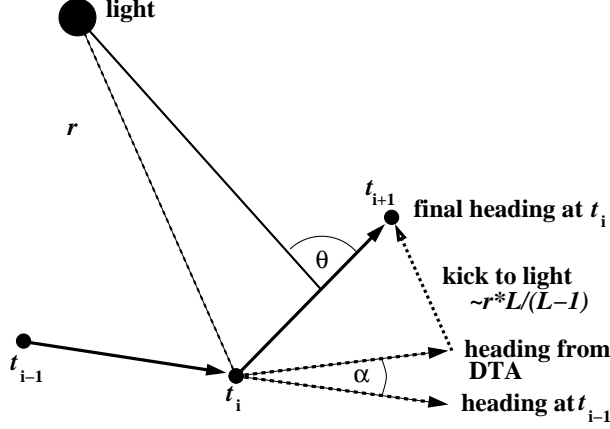


Fig. 17. The geometry of a pair of iterations, t_i and t_{i+1} , of the RWT showing distance to the light source r , heading angle θ , and turning angle α , as taken from the DTA shown in Fig. 16.

With the RWT outlined above, the moves of the walker can be simulated for varying attraction strength L . For $L \cong 0.4$ the walker revolves around the light source in both directions and frequently changes its rotational direction similar to the recorded *Daphnia* motions shown in Fig. 8. Thus the RWT predicts limit cycle motions similar to those of the ABP theory. For smaller values of L , the circular motion is less pronounced as the influence of the randomness increases. For larger L , the circling breaks down and the walker mainly steps back and forth over the light source. This simulates the noisy fixed point motions similar to those predicted by the ABP theory. But in the RWT, the strength of attraction to light governs the type of movement. That is, in the RWT, the shape of the potential varies while the self-propelling velocity is constant. Whereas, in the ABP theory, the shape of the potential is fixed while the self-propelling velocity varies (this velocity is determined by the parameters of the energy depot and the friction coefficient).

We turn now to measures of average quantities as predicted by the RWT. As in the experiment discussed in Section 4, rotational motion is demonstrated by the distribution of heading angles, $P(\theta)$. The model predicts a similar distribution with equally probable rotational motions in both directions as shown in Fig. 18(a) for several values of the light strength, L . The distribution of radii, $P(r)$, is shown in Fig. 18(b) again for the same set of values of L . Fig. 18(c) displays the average number of iterations $\langle M_C \rangle$ before a change in the circling direction for different L . A maximum at $L = 0.4$ implies that the most pronounced circling takes place at this intermediate value of the attraction strength. Figure 18(d) shows the angular momentum distribution, $P(L_{\text{ang}})$ for this optimal value of L . Finally, the distribution $P(M_C)$ of the number of hops (iterations) before a reversal of direction is shown in Fig. 18(e), again for $L = 0.4$. For comparison of the simulation results to the experimental data see the figures in Section 4. A more detailed discussion of these results can be found in Ordemann et al. (2003b).

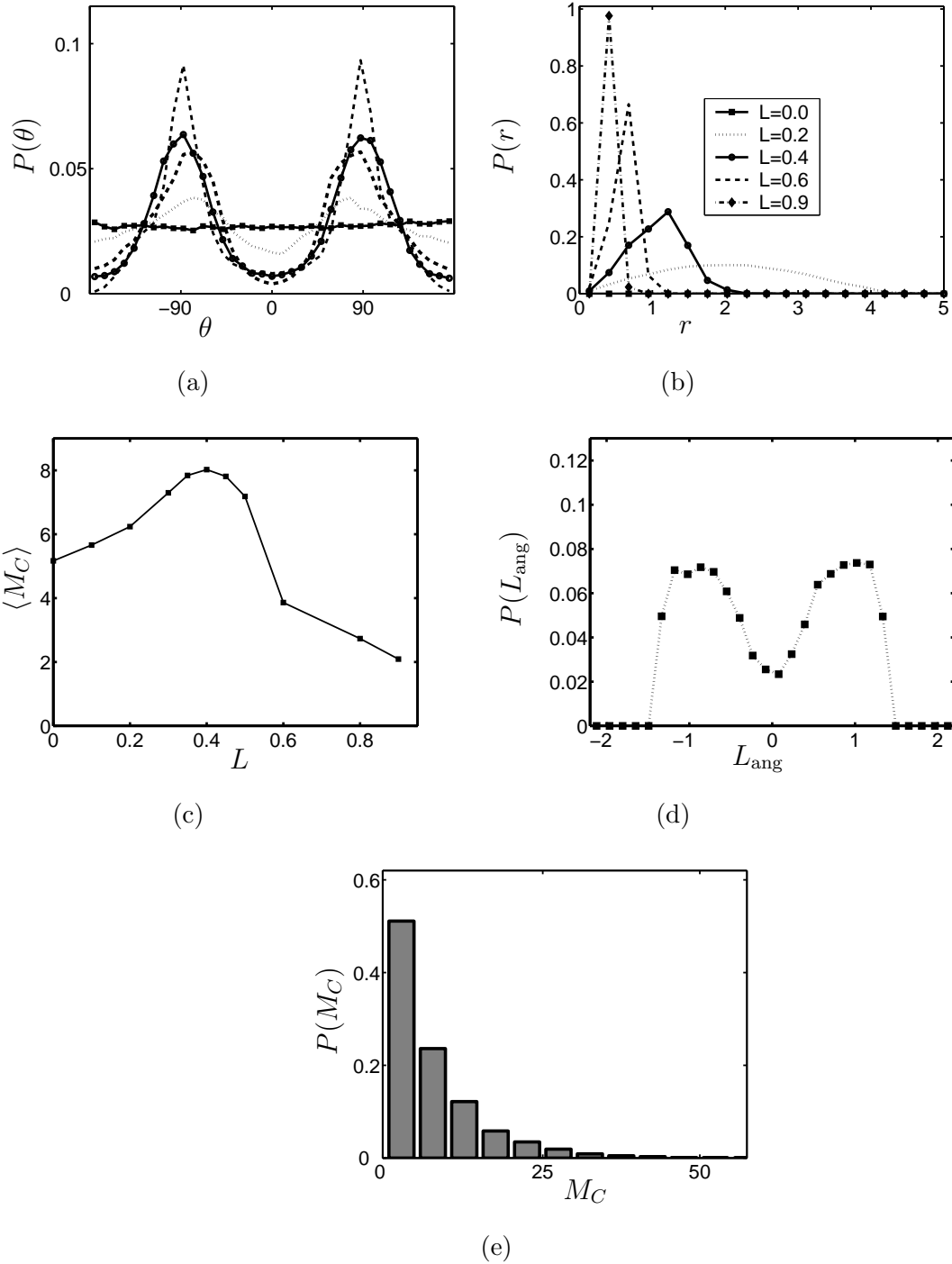


Fig. 18. Statistical measures predicted by the RWT for $L = 0.0$ (black squares), 0.2 (dotted line), 0.4 (black circles), 0.6 (dashed line), and 0.9 (black diamonds), see also inset of (b). (a) The distribution of heading angles, $P(\theta)$. The twin maxima at $\pm 90^\circ$ demonstrate equally probable rotational motions in both directions (CW and CCW). (b) The distribution of radii, $P(r)$. (c) The average number of iterations $\langle M_C \rangle$ before a change in the circling direction takes place for different L . Note the maximum at $L = 0.4$ indicating the case of most pronounced circling. (d) The distribution of angular momentum, $P(L_{\text{ang}})$, and (e) the distribution of the number of hops before a change of rotational direction, $P(M_C)$, both at $L = 0.4$. Plots are adapted from Ordemann et al. (2003b,c).

8.4 Diffusion in RWT I

We can study the natural diffusion of *Daphnia* by once again considering their motions in the dark. Within the framework of the RWT, a convenient measure of diffusion with time, is the end-to-end distance R . This is the straight-line (Euclidean) distance from the starting point of a walkers trajectory to the end point at the time t_i . Of course, an ensemble average of such distances must be obtained from a large number of trajectories, each generated with a different seed for the random number generator. Of interest is the exponent, ν , defined by $\langle R^2 \rangle^{\frac{1}{2}} \propto t^\nu$, where t is the time (or the number of iterations) after the walker is started, and the angular brackets indicate the aforementioned ensemble average (see for example Hughes, 1995). For purely Brownian particles, that is those with zero correlation, $\nu = 1/2$. In contrast, for our particles with a temporal short-range positive correlation, we find $\nu = 1$ for short time scales, followed by a crossover to $\nu = 1/2$ for asymptotically long times. This is shown by the simulation results (full circles) in Fig. 19. In general, for short-

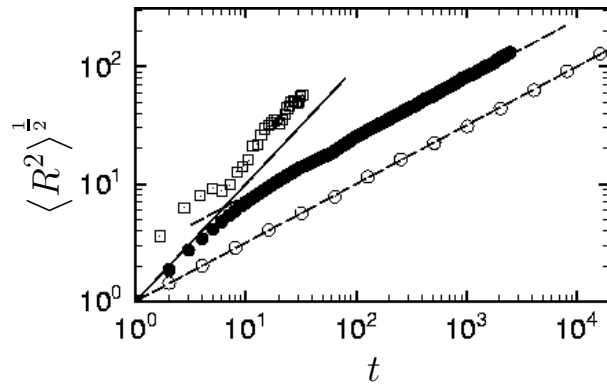


Fig. 19. Diffusion of *Daphnia* and of random walkers with and without short time correlations. The root mean square (rms) end-to-end distance $\langle R^2 \rangle^{\frac{1}{2}}$ is plotted versus time, t . For the simulations, 500 realizations were used with a one step correlation (full circles) and zero correlation (open circles). The experimental data (open squares) was obtained from the trajectories of eight *Daphnia*, where the distances are in mm and the time is in sec. The slope of the dashed line is 1 and of the solid lines 1/2, indicating ballistic (correlated) and uncorrelated motions, respectively.

range temporal correlations, the crossover time from non-Brownian motion to Brownian motion depends on the magnitude of the correlation time (memory). Here the correlation time is just one time step, since we simply update the turning angle according to the DTA at each iteration. For comparison, we show a simulation for purely Brownian walkers (open circles in Fig. 19) for which $\nu = 1/2$ always. When calculating the rms end-to-end distance of *Daphnia* motions in the dark, we observe an exponent $\nu \cong 1$ for $t \leq 30\text{sec}$ (see squares in Fig. 19). Thus their motions are governed by positive correlations at least for short time scales (for more details see Ordemann et al., 2003c). It is widely assumed that

for long time scales, that require much larger water reservoirs, the tracks of zooplankton in the field resemble Brownian motion, in agreement with our simulation at long times. Unfortunately, we were unable to observe the crossover experimentally, because we cannot record long enough trajectories. The trajectory length was limited by the size of our aquarium and by the available field of view in respect to the resolution of the video cameras.

8.5 Diffusion in RWT II

As has been observed in the experiments *Daphnia* tend to turn with a preferred angle at every hop they make (see Fig. 16). The question which occurs, having this in mind, is: Why do *Daphnia* hop with an DTA as shown above? What could be an reason for it? Can it be an evolutionary one? In order to answer this question it is reasonable to calculate the diffusion coefficient, having the aforementioned DTA in mind, and compare this with normal Brownian motion as it has been done in Komin et al. (2004). In order to calculate the diffusion coefficient we derive the mean square displacement of a swarm after $n = t/\Delta t$ time steps:

$$\langle R_n^2 \rangle = n\Delta x^2 + 2\Delta x^2 \sum_{i=1}^{n-1} \sum_{j>1}^n \langle \cos \alpha \rangle, \quad (12)$$

which depends on the angular correlation function:

$$C_\alpha = \langle \cos \alpha \rangle = \int_{-\pi}^{\pi} P(\alpha) \cos \alpha d\alpha. \quad (13)$$

After some transformations (Okubo and Levin, 2001; Wu et al., 2000) of Eq. (12) the mean squared displacement of a two-dimensional correlated random walk can be calculated what leads to the diffusion coefficient (Komin et al., 2004):

$$4D = \frac{1 + C_\alpha}{1 - C_\alpha} \frac{\Delta x^2}{\Delta t}. \quad (14)$$

As Eqs. (12) and (14) show the angular correlation function is crucial for the behavior of the time evolution of the mean square displacement of the particles and therefore for the diffusion behavior. If $0 < C_\alpha < 1$ the diffusion would be enhanced. This could be compared with a mean turning angle $0 < \alpha < \pi/2$, as observed with the *Daphnia*. In Komin et al. (2004) C_α has been calculated analytically assuming the DTA can be approximated by a Gaussian distribution (shown in Fig. 20). For $\langle \alpha \rangle = \pi/2$ we have a $C_\alpha = 0$ and therefore

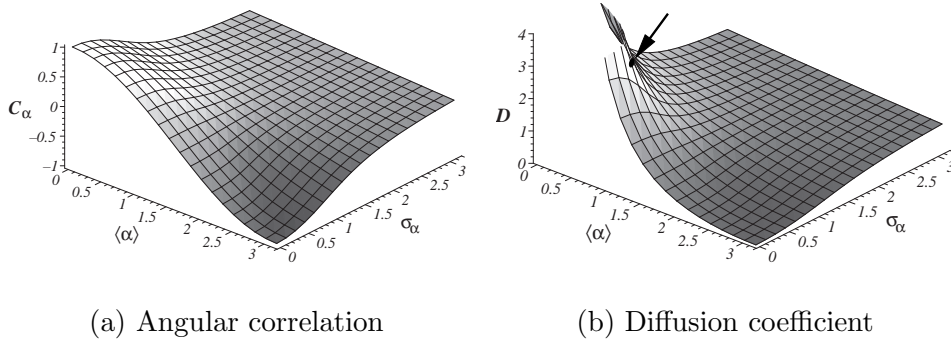


Fig. 20. (a) Angular correlation versus mean $\langle\alpha\rangle$ and variance σ_α of a Gaussian like DTA. (b) Diffusion coefficient. The parameters out of the *Daphnia* experiments are indicated with an arrow at the following values: $\langle\alpha\rangle = 0.84$, $\sigma_\alpha = 0.63$ and $D = 3.1$.

$D = 1$, what is equivalent to free diffusion, and does not depend on the standard deviation of the turning angle anymore.

Taking the experimental parameters for the *Daphnia* looking at Fig. 20(b) it seems to be obvious that the DTA for zooplankton has evolutionary advantages. The diffusion is enhanced and therefore an animal is able to cover a larger area while foraging for food.

8.6 Breaking the Symmetry in the RWT

We now turn to a simulation of the transition to vortex viewed as a phase transition within the context of our RWT model. The model is modified based on ideas about hydrodynamic feedback. We assume that the *Daphnia* are sensitive to small water movements, and that they have a tendency to align the direction of their motions with that of the majority of their neighbors. We thus define a global order parameter, $O = (N_{CW} - N_{CCW})/N_{tot}$, where N_{CW} and N_{CCW} are the instantaneous number of particles moving CW and CCW, respectively, and N_{tot} is the total number of particles. Particles are considered to be executing rotational motion if the absolute value of their heading angles lies within the range, $80 \leq |\theta| \leq 100$. In the simulation, O evolves with time. It is zero at instants when there is no net directional motion of the particles, smaller or larger than zero when there is net CCW or CW motion respectively. For the fully formed vortex (all particles moving in the same direction), $O \rightarrow \pm 1$.

We now focus on motions in a small neighborhood of radius a , supposing that a single *Daphnia* can sense hydrodynamic disturbances only from its neighbors. Motions within the neighborhood of a particle are governed by a local order parameter, $V = (A_{CW} - A_{CCW})/N_a$, where A_{CCW} and A_{CW} are the numbers

of particles within the neighborhood that satisfy the same definition of rotational motion, and N_a is the number of all particles within the neighborhood. In addition to the kick toward the light that applies to all particles in the simulation, we now include a local kick, $K = qV$ in the appropriate direction (CW for $V > 0$, CCW for $V < 0$) to the corresponding particle. Depending on the strength, q , of the kick and the size of the neighborhood, a vortex forms after a certain time. The formation of the vortex can be tracked by observing the temporal evolution of the global order parameter O . An example is shown in Fig. 21.

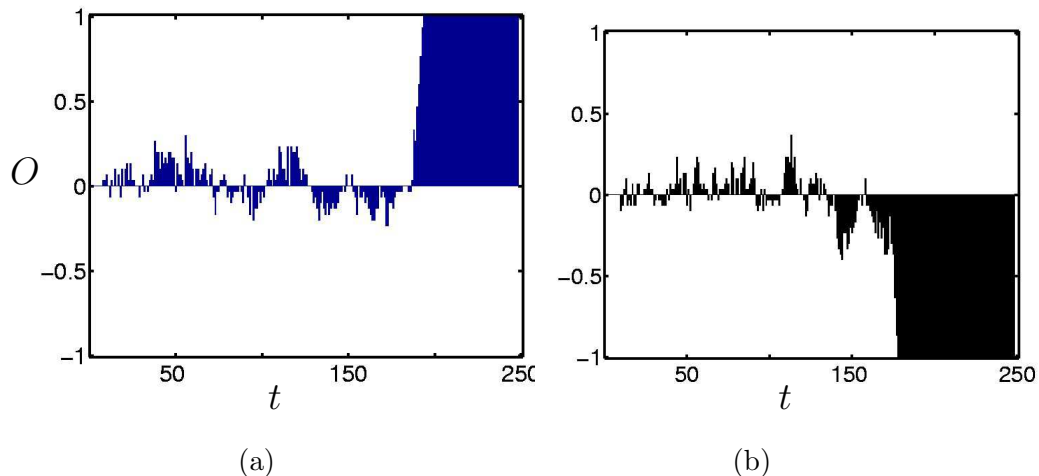


Fig. 21. Evolution of the global order parameter, O , showing the formation of the vortex (a) in CW direction ($O \rightarrow +1$) at $t \simeq 190$ time steps for parameters, $N_{\text{tot}} = 30$, $a = 0.7$, and $q = 0.16$, (b) in CCW direction ($O \rightarrow -1$) at $t \simeq 180$ time steps for the same parameters.

9 Discussion and Conclusions

Daphnia provide for the first time, the opportunity to construct well-controlled laboratory experiments with real biological agents. Such experiments provide crucial tests of existing different theoretical models of swarming, fixed point and rotational motions and vortex formation. And therefore these experiments open up the possibility to learn more about the aforementioned four different animal and agent motions through the interplay of theoretical modeling and experimental investigations. For *Daphnia*, the interaction that leads to swarming and vortex formation is not a direct one, as is the case for birds and fish that almost certainly use visual velocity alignment. Moreover, *Daphnia* swarms do not perform obvious predator avoidance maneuvers such as swarm splitting and recombining (Hall et al., 1986). Nevertheless, the observation of vortex-swarming by *Daphnia* in the laboratory provides the possibility to learn

more about the physical, chemical and biological aspects of this phenomenon that may be important for understanding similar motions exhibited by other living creatures. Further experiments with *Daphnia* will be necessary to understand in detail the factors that influence vortex-swarming, for example, *Daphnia* species, predator kairomone concentration, density of both food and individuals, and light intensity and wavelength. Light patterns and their perception by *Daphnia* as well as the physical aspects of the bio-hydrodynamic vortex need more attention.

The ABP model assumes that particles can absorb energy distributed over a medium in which they move and store it in a depot in a way similar to animals actively foraging for food over some space. Like animals, the particles must expend energy in order to move through the medium, and they experience a velocity-dependent dissipation. Also they expend energy to stay alive (similar to metabolism). Furthermore, also like real animals, they are subject to variable (random) forces, or “noise”. A confining potential is added in order that the particles are confined (or swarm). The model is therefore well motivated from a biological point of view. Interestingly, in addition to swarming, it predicts two basic motions that we designate the noisy fixed point and the equally probable, symmetric limit cycle pair. Similar motions are commonly observed in a variety of animals ranging in size and complexity from bacteria to birds and fish. Moreover, the ABP model has taught us that these two canonical particle motions arise from a minimal set of conditions. The particles must exhibit a mean self-propelling velocity and they must be confined either by an external potential or by the mean field that arises from an interparticle attractive interaction. Our experiments with small densities of *Daphnia* demonstrate the two basic motions. Moreover, the two limit cycles form the skeleton from which the vortex is built after some symmetry-breaking process eliminates one in favor of the other. At large particle densities the APB model was extended to include symmetry breaking by Oseen hydrodynamic flow in one instance and by an interparticle avoidance process, modeled by including a short range repulsive potential, in another. Both processes lead to vortex formations, similar to those observed with high density *Daphnia* swarms, but it remains to investigate which one better describes the experimental observations.

The model described by the RWT has also taught us something significant. Without including the peaked DTA, that signifies a statistical bias in favor of forward motion, in the model, no limit cycle motions of the walkers develop for any value of light intensity. With a uniform distribution of turning angles (uncorrelated Brownian walkers), only noisy fixed point motion is possible. Thus short-range temporal correlations, here indicated by the twin peaks in the DTA, are necessary for rotational motions about the central attractant. Within the framework of the RWT, we can now list four minimal conditions necessary to form vortices: i) a self-propelling mean velocity, ii) a statistical bias in favor of forward motion, iii) a central attractant, and iv) a symmetry

breaking process that tends to align local velocities. The bimodal DTA, necessary for rotational motion, might be an essential ingredient of the collective motions of large colonies of creatures and thus might be a general feature detectable in other animals as well. Why the natural movement of plankton follows such a distribution with maxima located at approximately $\pm 35^\circ$ (true for both our *Daphnia* and ocean-going zoo plankton) and how the animals actually choose to turn either left or right at the end of each hop are unanswered questions. But it is intriguing to speculate that these preferred turning angles may somehow enhance fitness, for example by possibly maximizing the acquisition of energy when food is distributed in patches. Indeed, we have calculated the diffusion coefficients for a swarm of random walkers using the experimentally determined bimodal DTA and found that, for parameters appropriate to the *Daphnia*, diffusion is considerably enhanced over what one would obtain for a walker with purely uncorrelated motions. This strongly suggests that motions characterized by a preferred turning angle confer an evolutionary advantage on foraging animals.

Acknowledgments

Supported by the Collaborative Research Center “Complex Nonlinear Processes” of the German Science Foundation, DFG-SFB555 (UE, WE, LSG) and the U.S. Office of Naval Research, Physical Sciences Division (FM). AO gratefully acknowledges financial support from a Feodor-Lynen Fellowship sponsored by the Alexander von Humboldt Foundation. FM is grateful to the US-ONR and to the Alexander von Humboldt Foundation for continuing support. AO and FM also wish to acknowledge Winfried Lampert for his patient tutorials and continuing encouragement throughout the course of this work. We are also grateful to J. Rudi Strickler and Ai Nihongi for stimulating discussions as well as their kind hospitality and for allowing us to further explore the motions of *Daphnia* in his laboratory. We thank David Russell, Beatrix Beisner, Allan Tessier and Lon Wilkens for valuable suggestions concerning zooplankton culture and behavior and help with the experimental set-up. We are indebted to Gabor Balázsi and Daniel Pflugfelder for some simulations and for initial help with the RWT. UE and LSG acknowledge the fruitful discussions with Igor M. Sokolov and Niko Komin concerning RWT and anomalous diffusion.

References

- Aronson, L. R., Tobach, E., Rosenblatt, J. S., Lehrman, D. S. (Eds.), 1972. Selected Writings of Theodore C. Schneirla, 1st Edition. W. H. Freeman

- and Co., San Francisco.
- Badoual, M., Jülicher, F., Prost, J., May 2002. Bidirectional cooperative motion of molecular motors. *Proceedings of the National Academy of Sciences USA* 99 (10), 6696–6701.
- Ben-Jacob, E., Cohen, I., Levine, H., 2000. Cooperative self-organization of microorganisms. *Advances in Physics* 49 (4), 395–554.
- Ben-Jacob, E., Shochet, O., Tenenbaum, A., Cohen, I., Czirók, A., Vicsek, T., 1994. Generic modelling of cooperative growth patterns in bacterial colonies. *Nature* 368, 46–49.
- Berg, H. C., 1993. *Random Walks in Biology*. Princeton University Press, Princeton.
- Bonner, J. T., Aug. 1998. A way of following individual cells in migrating slugs of *Dictyostelium discoideum*. *Proceedings of the National Academy of Sciences USA* 95, 9355–9359.
- Buchanan, C., Goldberg, B., 1981. The action spectrum of *Daphnia magna* (Crustacea) phototaxis in a simulated natural environment. *Journal of Photochemistry and Photobiology* 34, 711–717.
- Buskey, E. J., Peterson, J. O., Ambler, J. W., 1996. The role of photoreception in the swarming behavior of the copepod *Dioithona oculata*. In: Lenz et al. (1996).
- Camazine, S., Deneubourg, J.-L., Franks, N. R., Sneyd, J., Theraulaz, G., Bonabeau, E., 2001. *Self-Organization in Biological Systems*. Princeton University Press, Princeton and Oxford.
- Caraco, T. S., Martindale, S., Pulliam, H. R., 1980. Avian flocking in the presence of a predator. *Nature* 285, 400–401.
- Couzin, I. D., Krause, J., James, R., Ruxton, G. D., Franks, N. R., 2002. Collective memory and spatial sorting in animal groups. *Journal of Theoretical Biology* 218, 1–11.
- Czirók, A., Ben-Jacob, E., Cohen, I., Vicsek, T., Aug. 1996. Formation of bacterial colonies via self-generated vortices. *Physical Review E* 54 (2), 1791–1801.
- Dao, D. N., Kessin, R. H., Ennis, H. L., 2000. Developmental cheating and the evolutionary biology of *Dictyostelium* and *Myxococcus*. *Microbiology* 146, 1505–1512.
- Dodson, S. I., 1996. Optimal swimming behavior of zooplankton. In: Lenz et al. (1996).
- Ebeling, W., Schweitzer, F., 2001. Swarms of particle agents with harmonic interactions. *Theory in Biosciences* 120 (3-4), 207–224.
- Ebeling, W., Schweitzer, F., Tilch, B., 1999. Active Brownian particles with energy depots modelling animal mobility. *BioSystems* 49, 17–29.
- Erdmann, U., 1997. Structure formation by Active Brownian particles with nonlinear friction. *Interjournal of Complex Systems* 114, reprint: Erdmann (2000).
- URL <http://www.interjournal.org>
- Erdmann, U., 2000. Structure formation by active brownian particles with

- nonlinear friction. In: Bar-Yam, Y. (Ed.), *Proceedings from the International Conference on Complex Systems on Unifying Themes in Complex Systems*. New England Complex Systems Institute Series on Complexity. Perseus Books, Cambridge, Massachusetts, pp. 153–161.
- Erdmann, U., Ebeling, W., 2003. Collective motion of brownian particles with hydrodynamic interactions. *Fluctuation and Noise Letters* 3 (2), L145–L154.
- Erdmann, U., Ebeling, W., Anishchenko, V. S., Jun. 2002a. Excitation of rotational modes in two-dimensional systems of driven brownian particles. *Physical Review E* 65, 061106.
- Erdmann, U., Ebeling, W., Mikhailov, A. S., Oct. 2002b. Noise induced transition from translational to rotational motion of swarms, preprint.
- Erdmann, U., Ebeling, W., Schweitzer, F., Schimansky-Geier, L., 2000. Brownian particles far from equilibrium. *European Physical Journal B* 15 (1), 105–113.
- Falkenhagen, H., 1971. *Theorie der Elektrolyte*. S. Hirzel Verlag, Leipzig, with the collaboration of Werner Ebeling.
- Flierl, G., Grünbaum, D., Levin, S. A., Olson, D., 1999. From individuals to aggregations: the interplay between behavior and physics. *Journal of Theoretical Biology* 196, 397–454.
- Gerritson, J., Strickler, J. R., 1977. Encounter probabilities and community structure in zooplankton: a mathematical model. *Journal of the Fisheries Research Board Canada* 34, 73–82.
- Hall, S. J., Wardle, C. S., MacLennan, D. N., 1986. Predator evasion in a fish school: test of a model of the fountain effect. *Marine Biology* 91, 143–148.
- Hamilton, W. D., 1971. Geometry for the selfish herd. *Journal Theoretical Biology* 31, 295–311.
- Haury, L. R., Yamazaki, H., 1995. The dichotomy of scales in the perception and aggregation behavior of zooplankton. *Journal of Plankton Research* 17, 191–197.
- Helbing, D., Molnár, P., 1995. Social force model for pedestrian dynamics. *Physical Review E* 51 (5), 4282–4286.
- Helbing, D., Molnár, P., Schweitzer, F., 1994. Computer simulations of pedestrian dynamics and trail formation. In: *Evolution of Natural Structures: Proceedings of the 3rd International Symposium of the SFB 230*. Vol. 9 of *Mitteilungen des SFB 230*. Stuttgart, pp. 229–234, reprint: <http://arxiv.org/abs/cond-mat/9805074>.
- Horsthemke, W., Lefever, R., 1984. *Noise-Induced Transitions: Theory and Applications in Physics, Chemistry and Biology*. Springer, Berlin.
- Hubbard, J. B., Douglas, J. F., 1993. Hydrodynamic friction of arbitrarily shaped brownian particles. *Physical Review E* 47 (5), R2983–R2986.
- Hughes, B. D., 1995. *Random Walks*. Vol. 1 of *Random Walks and Random Environment*. Oxford University Press, Oxford.
- Humphries, D. A., Driver, P. M., 1967. Erratic display as a defense against predators. *Science* 156, 1767–1768.
- Huth, A., Wissel, C., 1990. The movement of fish schools: A simulation model.

- In: Alt, W., Hoffmann, G. (Eds.), Biological Motion. Vol. 89 of Lecture Notes in Biomathematics. Springer, Berlin, pp. 578–590.
- Jakobsen, P. J., Birkeland, K., Johnsen, G. H., 1994. Swarm location in zooplankton as an anti-predator defense mechanism. *Animal Behaviour* 47 (1), 175–178.
- Jakobsen, P. J., Johnsen, G. H., 1988. The influence of food limitation on swarming behaviour in the waterflea *Bosmina longispina*. *Animal Behaviour* 36, 991–995.
- Jensen, K. H., Jakobsen, P. J., Kleiven, O. T., 1998. Fish kairomone regulation of internal swarm structure in *Daphnia pulex* (Cladocera: Crustacea). *Hydrobiologia* 368, 123–127.
- Jülicher, F., Ajdari, A., Prost, J., Oct. 1997. Modeling molecular motors. *Review of Modern Physics* 69 (4), 1269–1281.
- Kittel, C., July 1995. Introduction to Solid State Physics, 7th Edition. Wiley Text Books. John Wiley & Sons, New York.
- Komin, N., Erdmann, U., Schimansky-Geier, L., 2004. Random walk theory applied to *Daphnia* motion. *Fluctuation and Noise Letters* In print.
- Kvam, O., Kleiven, O. T., 1995. Diel horizontal migration and swarm formation in *Daphnia* in response to *Chaoborus*. *Hydrobiologia* 307, 177–184.
- Landau, L. D., Lifschitz, E. M., Jul. 1987. Fluid Mechanics, 2nd Edition. Vol. 6 of Course of Theoretical Physics. Butterworth-Heinemann, Burlington MA.
- Larkin, R., Frase, B., 1988. Circular paths of birds flying near a broadcasting tower in cloud. *Journal of Comparative Psychology* 102, 90–93.
- Larsson, P., Dodson, S., 1993. Chemical communication in planktonic animals. *Archiv für Hydrobiologie* 129, 129–155.
- Lenz, P. H., Hartline, J. E., Purcell, J. E., Macmillan, D. L. (Eds.), 1996. Zooplankton: Sensory Ecology and Physiology. Gordon & Breach, Amsterdam.
- Levine, H., Rappel, W.-J., Cohen, I., Jan. 2001. Self-organization in systems of self-propelled particles. *Physical Review E* 63, 017101.
- Levine, H., Reynolds, W., May 1991. Streaming instability of aggregating slime mold amoebae. *Physical Review Letters* 66 (18), 2400–2403.
- Lobel, P. S., Randall, J. E., 1986. Swarming behavior of the hyperiid amphipod *Anchylomera blossevilli*. *Journal of Plankton Research* 8, 253–262.
- Mach, R., Ordemann, A., Schweitzer, F., 2003. Modeling vortex swarming in *Daphnia*, preprint.
- Morse, P. M., 1929. Diatomic molecules according to the wave mechanics. ii. vibrational levels. *Physical Review* 34 (1), 57–64.
- Morse, P. M., Stueckelberg, E. C. G., 1929. Diatomic molecules according to the wave mechanics i: Electronic levels of the hydrogen molecular ion. *Physical Review* 33 (6), 932–947.
- Neelov, I. M., Adolf, D. B., Lyulin, A. V., Davies, G. R., Aug. 2002. Brownian dynamics simulation of linear polymers under elongational flow: Bead rod model with hydrodynamic interactions. *Journal of Chemical Physics* 117 (8), 4030–4041.
- Nihongi, A., Ordemann, A., Lovern, S., Strickler, J. R., 2003. Fish kairomones

- can induce spinning behavior in *Daphnia pulex* in the dark, preprint.
- Nihongi, Ai, 2002. private communication.
- Niwa, H.-S., 1994. Self-organizing dynamic model of fish schooling. *Journal of Theoretical Biology* 171, 123–136.
- Niwa, H.-S., 1996. Newtonian dynamical approach to fish schooling. *Journal of Theoretical Biology* 181, 47–63.
- Okubo, A., Levin, S. A., 2001. *Diffusion and Ecological Problems: Modern Perspectives*, 2nd Edition. Vol. 14 of *Interdisciplinary Applied Mathematics*. Springer, New York.
- Ordemann, A., Balazsi, G., Caspari, E., Moss, F., Jun. 2003a. *Daphnia* swarms: from single agent dynamics to collective vortex formation. In: Bezrukov, S. M., Frauenfelder, H., Moss, F. (Eds.), *Fluctuations and Noise in Biological, Biophysical, and Biomedical Systems*. Vol. 5110 of *Proceedings of SPIE*. SPIE, Bellingham, pp. 172–179.
- Ordemann, A., Balazsi, G., Moss, F., 2003b. Motions of *Daphnia* in a light field: Random walks with a zooplankton. *Nova Acta Leopoldina* 87 (328), in press.
- Ordemann, A., Balazsi, G., Moss, F., Jul. 2003c. Pattern formation and stochastic motion of zooplankton *Daphnia* in a light field. *Physica A* 325 (1-2), 260–266.
- Oseen, C. W., 1915a. Beiträge zur Hydrodynamik I. *Annalen der Physik* 46 (2), 231–252.
- Oseen, C. W., 1915b. Beiträge zur Hydrodynamik II. *Annalen der Physik* 46 (5), 623–640.
- Oseen, C. W., 1915c. Beiträge zur Hydrodynamik III. *Annalen der Physik* 46 (8), 1130–1150.
- Parrish, J. K., Edelstein-Keshet, L., Apr. 1999. Complexity, pattern, and evolutionary trade-offs in animal aggregation. *Science* 284, 99–101.
- Parrish, J. K., Viscido, S. V., Grünbaum, D., Jun. 2002. Self-organized fish schools: An examination of emergent properties. *Biological Bulletin* 202, 296–305.
- Partridge, B. L., 1982. The structure and function of fish schools. *Scientific American* 246, 90–99.
- Pulliam, H. R., 1973. The advantage of flocking. *J. Theor. Biol.* 38, 419–422.
- Rappel, W.-J., Nicol, A., Sarkissian, A., Levine, H., Loomis, W. F., Aug. 1999. Self-organized vortex state in two-dimensional *Dictyostelium* dynamics. *Physical Review Letters* 83 (6), 1247–1250.
- Rayleigh, J. W. S., 1894. *The Theory of Sound*, 2nd Edition. Vol. I. MacMillan, London.
- Rhode, S. C., Pawlowski, M., Tollrian, R., 2001. The impact of ultraviolet radiation on the vertical distribution of zooplankton of the genus *Daphnia*. *Nature* 412 (6842), 69–72.
- Schienbein, M., Gruler, H., 1993. Langevin equation, Fokker-Planck equation and cell migration. *Bulletin of Mathematical Biology* 55, 585–608.
- Schimansky-Geier, L., Mieth, M., Rosé, H., Malchow, H., 1995. Structure for-

- mation by Active Brownian particles. *Physics Letters A* 207 (3-4), 140–146.
- Schmitt, F. G., Seuront, L., 2001. Multifractal random walk in copepod behavior. *Physica A* 301 (1-4), 375–396.
- Schweitzer, F., 2003. *Brownian Agents and Active Particles*. Springer Series in Synergetics. Springer, Berlin.
- Schweitzer, F., Ebeling, W., Tilch, B., Jun. 1998. Complex motion of Brownian particles with energy depots. *Physical Review Letters* 80 (23), 5044–5047.
- Smith, K. C., Macagno, E. R., 1990. UV photoreceptors in the compound eye of *Daphnia magna* (Crustacean, Branchiopoda). A fourth spectral class in single ommatidia. *Journal of Comparative Physiology A* 166, 597–606.
- Steuernagel, O., Ebeling, W., Calenbuhr, V., 1994. An elementary model for directed active motion. *Chaos, Solitons & Fractals* 4 (10), 1917–1930.
- Strickler, R., 1998. Observing free-swimming copepods mating. *Philosophical Transactions of the Royal Society London B* 353, 671–680.
- Timoshenko, E. G., Dawson, K. A., Jan. 1995. Equilibrium properties of polymers from the langevin equation: Gaussian self-consistent approach. *Physical Review E* 51 (1), 492–498.
- Toner, J., Tu, Y., Dec. 1995. Long-range order in a two-dimensional dynamical XY model: How birds fly together. *Physical Review Letters* 75 (23), 4326–4329.
- Toner, J., Tu, Y., Oct. 1998. Flocks, herds and schools: A quantitative theory of flocking. *Physical Review E* 58 (4), 4828–4857.
- Vicsek, T., Czirók, A., Ben-Jacob, E., Cohen, I., Shochet, O., Aug. 1995. Novel type of phase transition in a system of self-driven particles. *Physical Review Letters* 75 (6), 1226–1229.
- Weihs, D., Jan. 1973a. Hydromechanics of fish schooling. *Nature* 241 (5387), 290–291.
- Weihs, D., Sep. 1973b. Optimal fish cruising speed. *Nature* 245 (5419), 48–50.
- Wu, H.-L., Li, B.-L., Springer, T. A., Neill, W. H., 2000. Modelling animal movement as a persistent random walk in two dimensions: expected magnitude of net displacement. *Ecological Modelling* 132, 115–124.
- Young, S., Getty, C., 1987. Visually guided feeding behaviour in the filter feeding cladoceran, *Daphnia magna*. *Animal Behaviour* 35, 541–548.
- Young, S., Taylor, V. A., 1990. Swimming tracks in two cladoceran species. *Animal Behaviour* 39, 10–16.
- Zaret, R. E., 1980. The animal and its viscous environment. In: Kerfoot, W. C. (Ed.), *Evolution and Ecology of Zooplankton Communities*. University Press of New England, Hanover, pp. 3–9.
- Zaret, T. M., Suffern, J. S., 1976. Vertical migration in zooplankton as a predator avoidance mechanism. *Limnology and Oceanography* 21, 804–813.